The emerging role of α-synuclein truncation in aggregation and disease

Received for publication, January 15, 2020, and in revised form, May 13, 2020 Published, Papers in Press, May 18, 2020, DOI 10.1074/jbc.REV120.011743

Zachary A. Sorrentino[1,2] **and Benoit I. Giasson**[1,2,3,*]

From the [1]*Department of Neuroscience, the* [2]*Center for Translational Research in Neurodegenerative Disease, and the* [3]*McKnight Brain Institute, College of Medicine, University of Florida, Gainesville, Florida, USA*

Edited by Paul E. Fraser

α-Synuclein (αsyn) is an abundant brain neuronal protein that can misfold and polymerize to form toxic fibrils coalescing into pathologic inclusions in neurodegenerative diseases, including Parkinson's disease, Lewy body dementia, and multiple system atrophy. These fibrils may induce further αsyn misfolding and propagation of pathologic fibrils in a prion-like process. It is unclear why αsyn initially misfolds, but a growing body of literature suggests a critical role of partial proteolytic processing resulting in various truncations of the highly charged and flexible carboxyl-terminal region. This review aims to 1) summarize recent evidence that disease-specific proteolytic truncations of αsyn occur in Parkinson's disease, Lewy body dementia, and multiple system atrophy and animal disease models; 2) provide mechanistic insights on how truncation of the amino and carboxyl regions of αsyn may modulate the propensity of αsyn to pathologically misfold; 3) compare experiments evaluating the prion-like properties of truncated forms of αsyn in various models with implications for disease progression; 4) assess uniquely toxic properties imparted to αsyn upon truncation; and 5) discuss pathways through which truncated αsyn forms and therapies targeted to interrupt them. Cumulatively, it is evident that truncation of αsyn, particularly carboxyl truncation that can be augmented by dysfunctional proteostasis, dramatically potentiates the propensity of αsyn to pathologically misfold into uniquely toxic fibrils with modulated prion-like seeding activity. Therapeutic strategies and experimental paradigms should operate under the assumption that truncation of αsyn is likely occurring in both initial and progressive disease stages, and preventing truncation may be an effective preventative strategy against pathologic inclusion formation.

Neurodegenerative diseases, including Alzheimer's disease (AD), Parkinson's disease (PD), and Lewy body dementia (LBD), are collectively the leading cause of dementia worldwide with devastating human and economic costs (1, 2). There currently exist no disease modifying therapies that slow or prevent the onset of dementia in these diseases (2), and further research is needed to understand underlying pathophysiologic processes with the goal of identifying targets for therapeutic strategies. Common to most neurodegenerative diseases is the presence of amyloidogenic aggregates comprised predominantly of misfolded proteins of neuronal origins (3, 4); these diseases are typically classified based on the clinical presentations and identity of the misfolded proteins (3).

α-Synuclein (αsyn) is a 140-residue, 14.46-kDa protein that is predominantly found within the presynaptic region of neurons in the central nervous system, where it has important functions in vesicle trafficking (5, 6). Misfolding of this protein and consequent intracellular inclusion formation is a hallmark of the class of neurodegenerative diseases termed synucleinopathies, which includes PD, LBD, and multiple system atrophy (MSA) (7). αsyn isolated from these inclusions is misfolded into pathologic, β-sheet–rich polymers assembled into various oligomers or larger amyloidogenic fibrils (8–13), which collectively can contribute to neuronal toxicity and dysfunction along with prion-like progression of disease (11, 14, 15). In addition to polymerization, pathologic αsyn harbors extensive post-translational modifications (PTMs), including phosphorylation, truncation, ubiquination, nitration, sumoylation, and multiple others (16–18).

The consequences of misfolded oligomeric and fibrillar forms of αsyn in preclinical models have been extensively studied and reviewed elsewhere (11, 19, 20), and current evidence suggests that disease progression may be difficult to thwart once these forms of αsyn are widespread due to prion-like recruitment of endogenous αsyn into further pathologic forms that can spread within and between neuronal and glial cells in a vicious cycle (20, 21). A more attractive therapeutic target may be the dysfunctional processes resulting in initial αsyn misfolding and fibril formation through mechanisms such as aberrant αsyn PTMs if these occur early or are essential for disease progression. Some PTMs have been shown *in vitro* to alter the propensity of αsyn to form pathologic fibrils similar to those isolated from disease inclusions (18, 22), and corollary *in vivo* processes likely responsible for the appearance of these PTMs such as oxidative stress and impaired protein clearance pathways are demonstrable in animal models of synucleinopathy and tissue from diseased patients (23–25). Indeed, PTMs of αsyn are abundant in disease, with 90% or more of αsyn being phosphorylated at Ser-129 and 15–20% being C-terminally truncated within pathologic inclusion extracts (16, 17, 26–28). C-terminal truncation of αsyn may be particularly detrimental among PTMs, as it has been consistently demonstrated *in vitro* that C-truncated αsyn self-assembles into fibrils far more readily than full-length (FL) αsyn or even familial disease causing missense mutant forms of αsyn (17, 29–36). Proteolytic formation of truncated αsyn (32, 37–42), possibly promoted by impairment of proteostasis as in aging (43), may initiate inclusion pathology formation and progression. This review aims to

* For correspondence: Benoit I. Giasson, bgiasson@ufl.edu.

summarize the evidence for the accumulation of diverse types of truncated αsyn in disease, survey the physiological processes involved in their formation, and discuss the functional implications in the context of pathologic fibril formation, toxicity, and prion-like disease progression.

αsyn background

αsyn has structurally distinct regions important to function and disease

αsyn was first isolated from synaptic vesicles in the *Torpedo* fish and was termed "synuclein" when a homologous protein was detected in rat neuronal synaptic vesicles and nuclear envelopes (44). The majority of αsyn is in a cytoplasmic, soluble form as an intrinsically disordered protein (6); in association with synaptic vesicles, the repeat-rich N terminus (residues 1–60) and "nonamyloid component" (NAC) domain (residues 61–95) adopt a helical structure necessary for the regulatory role of αsyn in vesicle trafficking that is thought to be a main function of αsyn in the neuron (45, 46). However, αsyn also functions in synaptic maintenance and SNARE protein assembly, as evidenced by its ability to mitigate phenotypes in CSPα null mice (47), and αsyn can function as a chaperone, which is made possible by labile intermolecular interactions inherent to unstructured proteins (48, 49). These biological functions of αsyn are attributed to its three overarching structural domains: the amphipathic N terminus, the hydrophobic NAC, and the acidic C terminus (residues 96–140). The N terminus harbors most of the seven imperfect KTKEGV 11-mer repeats important in helix formation in association with phospholipid surfaces (45, 46). The NAC region is hydrophobic and acts as a lipid "sensor," mediating specificity for synaptic vesicle binding (5, 45). Last, the C terminus remains unstructured in nearly all conformations due to its highly charged 15 acidic residues; the charged state and ever-changing structure of this region permits most of the chaperone activity of αsyn along with its ability to bind metals, polyamines, and positively charged proteins such as tau (5, 45, 48, 50, 51).

Due largely to the hydrophobic nature of the NAC region (52), a confluence of pathologic processes can result in the disease-associated misfolding of αsyn into dense fibrils that are highly insoluble in detergents (8). Using proteolytic digestion of fibrils, antibody accessibility, and structural techniques such as cryo-EM, it was determined that the typical αsyn amyloid fibril core is composed roughly of residues ~31–102 stacked as in-register β-sheets (31, 51, 53–59). The extreme N terminus and most of the C terminus are not within the amyloid core, but the N terminus is still relatively structured compared with the fully disordered C terminus (53, 55, 60). The C terminus may also govern higher-order assembly of fibrils, as its highly negative charge governs lateral packing of fibrils and possibly association of protofilaments into more mature amyloid species (33, 56, 60).

αsyn-laden inclusions are hallmarks in multiple neurodegenerative diseases

αsyn was first associated to neurodegenerative diseases when the NAC region of the protein was detected in association with amyloid plaques in AD (61, 62). A more direct involvement in neurodegenerative diseases was supported by the seminal discovery that the A53T missense mutation in the *SNCA* gene encoding αsyn was responsible for autosomal dominant PD in the Contursi kindred (63). Immediately thereafter, αsyn was identified as the major component of Lewy bodies (LBs) and Lewy neurites (LNs) that have been pathologic hallmarks in PD and LBD for 100 years prior (64, 65).

αsyn pathological inclusions are known to be present in a number of heterogeneous neurodegenerative diseases, including in about ~50% of AD patients (65–67). Symptomatically and pathologically, various diseases afflicted by αsyn inclusions can be very different. PD and LBD are pathologically akin with LB and LN pathology (Lewy-related pathology; LRP) prevalent in the degenerating dopaminergic neurons of the substantia nigra pars compacta (SNpc) that underlies the parkinsonism movement disorder (66, 68). In stark contrast to the aforementioned diseases where αsyn aggregates are mainly found in the neuronal cytoplasm as LBs and LNs, MSA is a movement disorder that may present with cerebellar signs or parkinsonism and is characterized by αsyn-containing glial cytoplasmic inclusions (GCIs) within oligodendrocytes (7, 66, 69). GCIs are predominantly formed in white matter tracts, but morphologically unique nuclear neuronal αsyn inclusions and neuronal cytoplasmic inclusions can also be found in various brain regions in MSA.

In the stereotyped pathologic progression of PD, αsyn inclusions are typically observed early in the peripheral nervous system (particularly in the gastrointestinal tract) and caudal brainstem coinciding with minor autonomic symptoms, followed by the onset of parkinsonism with aggregate formation and neurodegeneration in the SNpc, with telencephalic pathology and cortical symptoms such as dementia and psychosis occurring in late stage (65, 66). In LBD, progression of disease is more varied than PD in that LRP may appear in limbic and cortical regions earlier than in PD, resulting in more rapid onset of dementia that can even precede motor symptoms or SNpc pathology (66, 67). MSA has its own unique progression patterns, further demonstrating the variance in disease states induced by misfolding of the same protein (7, 66, 69). Additionally, ~40–60% of AD cases present LRP, often restricted to limbic regions, that bears similarities to that of PD and LBD, albeit with some differences (66, 67). There exist many other less common neurodegenerative diseases exhibiting diverse αsyn aggregates either as primary or secondary lesions with their own unique symptoms and progression patterns (65). In addition to the diversity in progression and morphology of αsyn inclusions between diseases and even across brain regions in the same disease, there is diversity in the cell types affected, as astrocytic and oligodendroglial αsyn pathologies are present in addition to neuronal αsyn aggregates in varying abundance, depending on the disease (21, 66, 67).

Variations among the synucleinopathies in terms of pathology, symptomatology, and rate of progression suggest that the form of pathologic αsyn present may differ between these diseases at the molecular level similar to the concept of strains in prion disease (20, 66, 70). Additionally, the pathologic and symptomatic progression of PD in particular seem to be linked

to the "spread" of pathologic αsyn aggregates through interconnected neurons in the autonomic nervous system, which again bears similarities to prion disease (71, 72). Indeed, much of the recent research on the molecular mechanisms of synucleinopathies is now based on the assumption that misfolded αsyn harbors prion-like activity.

Molecular mechanisms of αsyn aggregation, prion-like spread, and toxicity are key to understanding synucleinopathies

Aggregates comprised of misfolded αsyn are directly implicated in mechanisms of cytotoxicity and disease progression. Evidence for the toxic role of αsyn is supported to date by the identification of seven missense mutations in the SNCA gene resulting in autosomal dominant synucleinopathies with associated symptoms (73–75). These mutant forms of αsyn are thought to cause disease by either accelerating polymerization into oligomers/fibrils, altering the physiologic function of αsyn, or a mixture of these mechanisms (74, 76). Additionally, increased gene dosage through duplication or triplication of the SNCA gene similarly results in familial synucleinopathy (73, 74). In animal models, overexpression of αsyn and usage of aggregation-prone familial mutant forms such as A53T αsyn results in robust Lewy-like neuronal αsyn inclusions, neuronal death, and motor symptoms (77, 78). Increasing the tendency of αsyn to polymerize through mutation or increased gene dosage leads to disease in these familial cases, and in sporadic synucleinopathies, aggregation-promoting PTMs may play a similar role (22, 67).

The assembly of αsyn monomers into oligomeric species and eventually β-sheet–rich fibrils is important to the disease process; the formation and continued presence of αsyn oligomers and fibrils in inclusion-bearing cells has been directly implicated in neuronal and glial toxicity through a number of pathways, including impairment of axonal transport, blockage of lysosomal autophagy and other proteolytic pathways, mitochondrial toxicity and oxidative stress, synaptic dysfunction, and functional insufficiency of monomeric αsyn from its typical presynaptic location (reviewed in Refs. 19, 79, and 80). In addition to the direct toxic mechanisms of intracellular aggregated αsyn, neuroinflammation is induced by glial detection of the αsyn aggregates and cytotoxicity, which may result in further damage (reviewed in Refs. 21, 81, and 82). Although there is debate as to which form of misfolded αsyn (oligomers, protofibrils, fibrils, etc.) is the most toxic, it is likely that all of these species are present in diseased cells (80).

In addition to their purported toxicity, αsyn aggregates demonstrate prion-like induction of further αsyn pathology and progression of disease (83). It was suggested that αsyn could potentially act similar to a prion when it was found that fetal stem cell grafts placed into the brains of PD patients developed αsyn inclusions within the grafts, demonstrating that a "spread" of pathology had occurred (84, 85). Stemming from the in-register β-sheet structure of αsyn fibrils (58) and the intrinsic lability of monomeric αsyn in adopting diverse conformations necessary for its physiologic function, it became apparent from early *in vitro* observations that the addition of preformed αsyn fibril "seeds" to a solution of αsyn monomers could induce fibril elongation as monomers assume a pathologic β-sheet conformation induced from the exposed "templates" at the ends of the fibrils in a process termed "conformational templating" (13, 83, 86–88). This seeded templating process bears similarities to the protein misfolding cyclic amplification technique common to the prion field, and further prion-like properties of αsyn were quickly explored (89). The introduction of preformed αsyn fibrils (PFFs) to cultured cells expressing monomeric αsyn induced a polymerization phenomenon similar to that seen *in vitro* (90–94). In animal models, intracerebral or even peripheral injection of PFFs or human synucleinopathy brain lysate into rodents can robustly trigger the formation of LB-like pathology and motor symptoms, further corroborating the importance of prion-like conformational templating in synucleinopathies (20, 95–98). The prion-like theory of αsyn conformational templating may explain propagation of pathology in synucleinopathies, where for PD in particular it has been proposed that spread of fibrils through anatomic connections sufficiently predicts which regions of the brain will be stereotypically affected (the Braak staging schema) and subsequently when various symptoms will arise based on regions affected (71, 72, 99, 100). Indeed, experimentation in various preclinical models has demonstrated that even nanomolar quantities of αsyn fibrils are able to spread between neurons and even glial cells through multiple extracellular and intercellular uptake mechanisms (reviewed in Refs. 20 and 21), suggesting that the appearance of misfolded αsyn aggregates may be sufficient to kick start a vicious cycle of further αsyn aggregation and prion-like spread.

Pathologic αsyn adopts different strains that may underlie heterogeneity in disease

Like prions, misfolded αsyn within fibrils can also adopt varied conformations, which bear similarities to "strains" in prion disease whereby the unique conformations of misfolded prion protein can be propagated, resulting in characteristic pathologies and symptoms particular to the initiating strain (reviewed in Ref. 70). Strains may explain why aggregation of the same protein, αsyn, is able to cause a spectrum of diseases, each with overlapping but separate pathologies, symptoms, regional and cellular distribution of inclusions, and rates of progression (66).

Monomers of recombinant αsyn can be induced to form into PFFs similar to fibrils found in LBs when incubated with agitation for several days (31); it was noted that upon microscopic examination, extensive heterogeneity exists in the ultrastructural appearance of these PFFs, with some displaying helical periodicity of paired protofibrils, which others lack, hinting at the existence of differing strains of αsyn fibrils (31, 54, 57). Further experimentation *in vitro* demonstrated that modifying the buffer parameters used (pH, ionic strength, etc.) for PFF production results in PFFs with unique structural and biochemical characteristics stemming from the modified conformations of the misfolded αsyn monomers comprising the aggregates (58, 70, 101–105). In cellular and animal models, these variant PFFs can be functionally different in terms of their potency in seeding αsyn pathology, rate of disease progression, the cell types

they affect, and even the morphology of inclusions that result in mice injected with the variants PFFs, which is strongly reminiscent of differing diseases resulting from prion strains (14, 70, 103, 105).

Extending the strain concept to human disease, αsyn fibrils from MSA brain lysate have been compared with lysate from LBD and PD brains to investigate whether there are unique structural and functional differences in fibrils between these diseases (reviewed in Ref. 70). Structurally, there are purported differences in the biochemical and ultrastructural characteristics between αsyn fibrils derived from MSA and LBD/PD brains; MSA fibrils appear to have more "twisted" fibril variants characterized by undulating fibril width along their length, which may not be as prevalent in LBD/PD αsyn fibrils (10, 31). In addition, MSA αsyn fibrils can be more stable to protease digestion (106) and detergent extraction (107) and less stable in denaturation with specific solvents (105) and interact with protein aggregate binding dyes differently from LBD/PD αsyn fibrils (108), which cumulatively demonstrates significant biochemical, and possibly conformational, differences in the fibrils between these diseases. Additionally, αsyn inclusions between MSA and LBD/PD are not only different in their morphologies and cellular locations, but also in detection, as evidenced by monoclonal antibodies that selectively label αsyn in MSA inclusions over LBD/PD (106) and the Gallyas–Braak silver staining technique that detects MSA inclusions and not typically those of LBD/PD (109).

Experimentally, MSA αsyn fibrils appear to be up to 1000 times more potent in their prion-like activity compared with LBD/PD αsyn fibrils or any PFF variant as measured by the time to inclusion formation and disease onset, amount of pathology, and amount of insoluble αsyn formed in animal and cellular models injected with various disease lysates and PFFs (106, 110–113). In addition to the increased potency, MSA αsyn fibrils can impart their unique structural conformation in induced pathology measured in cell culture assays and passaging studies in mice (105, 106, 114). It is increasingly evident that different strains of αsyn fibrils likely contribute to the different synucleinopathies or even rates of progression within the same synucleinopathy; however, it is still not understood why specifically these different strains arise.

Mechanisms by which the differing strains of misfolded αsyn and subsequent fibrils could arise include modification of αsyn through PTMs or altered subcellular environment promoting certain conformations. It is likely that PTMs could induce unique αsyn strains, as even single residue mutations in αsyn are able to structurally alter resulting αsyn fibrils and functionally impact prion-like seeding and biochemical properties in cellular and animal models (115–118). Likewise, there exists a "species barrier" between mouse and human αsyn, where due to their 7-amino acid difference, fibrils comprised of the αsyn of one species do not seed monomers of the other species as efficiently due to presumed structural incompatibility (119–122). The majority of misfolded pathologic αsyn harbors PTMs such as phosphorylation at Ser-129 (pSer-129), and recent work is establishing the role of these PTMs in modifying prion-like seeding of αsyn fibrils. For pSer-129 in particular, two papers have observed that αsyn inclusions in MSA appear to be less reactive than LBD for common antibodies targeted against pSer-129, and biochemical analysis suggests less pSer-129 in the insoluble αsyn fibrils extracted from MSA brains, suggesting that differing PTMs may indeed result in different fibril strains (106, 123).

Experimentation using animal models to explore the effect of PTMs on aggregation is extensive, but far fewer studies have been conducted to determine how the presence of PTMs within αsyn fibrils impacts prion-like seeding (18). Compared with a single point mutation or phosphorylation site, removal of multiple residues through truncation of αsyn may have a large impact on prion-like seeding activity and strain-like alterations in structural and biochemical properties, which will be discussed herein to determine how the presence of this PTM in disease could impact progression.

Evidence for truncated αsyn in health and disease

Detection in human neurodegenerative diseases

Although truncation of αsyn may theoretically increase the propensity of the protein to aggregate into pathologic forms, it is important to first confirm that truncated αsyn is actually present in human disease and, if so, which specific ones. Note that post-mortem interval does not affect the observation of truncated αsyn, showing that truncation is not an artifact of post-mortem decay (16, 26, 124). Studies aiming to detect truncated forms of αsyn typically rely on immunoblotting, immunohistochemistry (IHC) with truncation-specific antibodies, or MS. Immunoblotting in the form of Western blotting (WB) is the most common method utilized; however, this analysis is not always straightforward, as human αsyn has an aberrant apparent mobility of ~19 kDa on SDS-PAGE compared with the predicted 14.4 kDa (6); thus, some truncations can result in unexpected shifts in mobility. In addition, the C-terminal truncation of αsyn removes acidic residues, resulting in an increased protein pI, and thus typical WB procedures may not detect the full extent of C-truncated forms of αsyn, as the pH levels of common blotting buffers are not ideal for the electrophoretic transfer onto membranes (22, 26, 125). The IHC approach that relies on antibodies specific for modified forms of the protein presents its own challenges, as it is difficult to produce antibodies specific for a truncated form of a protein without any cross-reactivity for the full-length form. MS avoids many of the shortcomings inherent to other techniques but is also the least common approach for detecting truncated αsyn. Despite these challenges, robust evidence exists that truncation of αsyn is occurring in a way that is largely disease-specific, and the estimated or exact truncated forms of αsyn identified are summarized in Table 1 (16, 17, 26–28, 62, 67, 124, 126–135). Overall, studies relating to truncated αsyn forms noted their presence on WB from LBD, PD, or MSA brain lysate; however, a few were particularly comprehensive in detecting their presence and attempting to identify exact truncation sites through the generation and IHC application of truncation-specific antibodies (16, 128–133) and MS (16, 27, 132, 134) to study diseased brain lysate.

In almost all studies utilizing WB of LBD and PD lysate, a common trend is observed where in the insoluble fraction

Table 1

Summary of observational studies of truncated αsyn in human synucleinopathies

The nomenclature for truncation when only approximate is indicated by a slash; 1–115/120 indicates C-terminal truncation occurred somewhere between residues 115 and 120.

Reference	Design	Identified truncations	Remarks
126	WB of MSA brains	~12-13 kDa	Strong 12 kDa band in MSA and not controls.
62	WB of LBD, PD brains	12 kDa 6 kDa	Both bands detected only with NAC antibody. 6 kDa more disease-specific.
28	WB of purified LBs from LBD, PD	14 kDa 16 kDa	14 kDa more abundant than FL (~19 kDa) in purified LBs.
127	WB of LBD, PD brains	15 kDa	15 kDa band C-truncated at indeterminate location. Most abundant in disease-associated detergent-insoluble fraction.
26	WB and MS of PD brains	12 kDa (1–119/125), 10 kDa, 8 kDa	12 kDa suggested to be truncated somewhere between 119-125; likely 1–119 and 1–122 from MS. 8 kDa band is both N- and C-truncated. 8 kDa most disease-specific. Up to 50% of αsyn truncated in PD-insoluble fraction.
17	WB of PD, LBD brains	~12 kDa (1–110/124), ~9 kDa (1–100/110), ~6 kDa (15/60-100/110)	6 kDa is N- and C-truncated. 6 kDa most disease-specific. ~15–30% of αsyn truncated in PD/LBD insoluble fraction.
16	WB and MS of LBD and PD brains; C truncation–specific antibody cleavage at residue 119 for LBD, PD, and MSA.	15 kDa (1–133/135), 13.5 kDa (1–126/129), 12.5 kDa (1–122), 12 kDa (1–119), 11.5 kDa (1–115), 10 kDa (1–96/105)	C truncation at 119 likely most common, but least specific for disease. C-truncated 119 αsyn found in LBs and GCIs. Other C truncations found only in insoluble fraction and disease-specific. All truncated αsyn examined had intact N terminus. 1–115, 1–119, 1–122, 1–133, and 1–135 αsyn confirmed with MS.
128	WB and protein sequencing of LBD and PD brains; IHC with truncation-specific/selective antibodies for cleavage at residue 9 or at 122	~10 kDa (10–122), ~12 kDa (1–122)	N-terminal truncation at residue 10 mainly detected LBs and not neuritic pathology; mainly central portion of LBs, suggesting role in early formation of LB. Truncated αsyn present in 70–90% of LBs. C-terminal truncation antibody (residue 122) had similar pattern and results to N-terminal truncation antibody staining.
129	WB and IHC of LBD and AD brains using truncation-specific antibodies for cleavage at residues 110 or 119	110 C-truncated αsyn, 119 C-truncated αsyn	119 C-truncated αsyn more common in LBs and LNs in LBD and AD brains than 110 C-truncated αsyn. Most LBs contained both FL and 119 C-truncated αsyn, and rarely only 119 αsyn. 110 C-truncated αsyn more specific for disease on WB than 119 αsyn.
124	WB of LBD brain extracts	~15 kDa (1–115/120), ~10 kDa, ~12 kDa	15 kDa band only truncation evident in soluble fraction of controls and LBD; epitope mapping suggests it is not N-truncated and is C-truncated between residues 115–122. 15 kDa band (likely 1–119) is enriched in the lysosomal fraction. 10 kDa and 12 kDa bands detected upon further subcellular purification of the cytosol. C-truncated αsyn enriched in center of LBs.
130	IHC of PD brains using truncation-specific antibodies for cleavage after residue 119 or 122	119 C-truncated αsyn, 122 C-truncated αsyn	C-truncated αsyn at residue 119 or 122 concentrated in the core of LBs and LNs; also found in pale bodies.
131	IHC and WB of LBD brains using truncation-specific antibody after residue 122	122 C-truncated αsyn	C-truncated αsyn at 122 increased in LBD compared with control brain lysate even in soluble fraction. IHC detected extensive 122 αsyn in dystrophic neurites and cortical LBs in the hippocampus and putamen
27	MS of PD brain lysate (frontal cortex)	In order of abundance: 5-140 > 1–122 > 1–119 > 1–135 > 39–140 > 68–140 Found in S.D.S insoluble fraction: 1–119, 1–135, 1–122, 5-140, 68–140	1–122, 1–135, and 1–119 truncated forms of αsyn had abundances of 0.23-0.26 compared with 1–140 αsyn in the SDS-insoluble fraction. Significant amounts of purely N-truncated αsyn detected.
132	MS, WB, and IHC with truncation-specific antibody at residue 103 for PD and LBD brains	1–103 C-truncated αsyn	1–103 αsyn present in both soluble and insoluble fractions of PD and LBD but not controls. Inclusions labeled in PD and LBD but not controls with the 103-specific antibody. Ratio of 1–103 αsyn to FL αsyn increased in SNpc relative to cortex in PD.
133	WB of PD brain lysate and IHC with antibody specific for pSer-129 only if also C-truncated	12.5 kDa (suggested to be residues 15–130), 25 kDa (dimer of truncated αsyn)	Particularly localized to mitochondria, where it exerts toxicity as small SDS-resistant aggregates. The 12.5 kDa band not detected by N- or C- terminal αsyn antibodies.
134	WB and MS of PD intestinal appendix lysate	1–125, 18–125, 19–125, 1–124, 18–124, 19–124, 1–114, 19–114, 19–115, 19–113 truncated αsyn	1–125, 1–124, and 19-125 appear to be particularly abundant. Significant increase in truncated αsyn in appendix compared with SNpc for the same brain and ratio of truncated to FL αsyn in appendix greatly increased for PD compared with controls.
67	WB of LBD lysate	~15 kDa C-truncated ~16 kDa C-truncated	Truncation bands mainly apparent in LBD insoluble fraction; some minor truncation bands in soluble fractions. More C-truncated αsyn in the amygdala/medial temporal lobe compared with cingulate.
135	IHC of PD SNpc and colon with truncation-specific antibody at residue 103	103 C-truncated αsyn	Usually co-located in inclusions with truncated tau. C-truncated 103 αsyn in SNpc and colonic neurons in PD and not controls.

containing aggregated αsyn there is a major ~17–19 kDa band representing FL αsyn; a ~12–15 kDa band only reactive to N-terminal αsyn antibodies, suggesting C-truncated forms of αsyn; and 1–2 additional minor bands of ~9–10 and ~6–8 kDa, which may be both N- and C-truncated αsyn (Table 1). Each truncation band seems to contain a mix of 2–3 truncated αsyn species that can be resolved using MS or specific antibodies. Confirmed C-truncated forms of αsyn found in detergent-

insoluble disease fractions studied by combinations of epitope mapping, MS, and/or truncation-specific antibodies end at residues 103, 110, 113, 114, 115, 119, 122, 124, 125, 133, and 135 (Table 1). Confirmed N-truncated forms of αsyn studied with similar techniques are those starting at residues 5, 10, 18, 19, and 68 (Table 1). In particular, 1–119 and 1–122 appear to be some of the most common forms of truncated αsyn and comprise the major portion of the ~12–15 kDa band; these have each been detected with multiple specific antibodies and MS experiments where their relative abundances were as high as 20–25% that of FL αsyn in the insoluble brain fraction (Table 1). The forms of αsyn truncated at only the extreme N or C terminus, such as 1–135 and 5–140, have also been determined to be highly abundant in two separate MS experiments (16, 27); however, they may not be distinguishable from FL αsyn on a typical WB due to size similarities and both becoming pSer-129–positive (16) (Table 1). A caveat to determining the most common truncated forms of αsyn is that each study often examined tissue from only one region, and the few studies that compared truncation in differing regions often demonstrated variation in the amount of truncated αsyn from one region to the next (67, 132, 134). It is difficult to arrive at even a rough number for the percentage of αsyn that is truncated in disease compared with controls due to the variety of truncated forms, regional variation, and detection issues; however, based only on the 2–3 major truncation bands visible on Western blots from multiple studies, it seems that ~15–30% of insoluble αsyn in PD/LBD is truncated (Table 1). Notably, almost all studies examining truncation have focused on LBD and PD and not MSA, although at least two studies have observed a ~12–15 kDa band in MSA and 119 C-truncated αsyn in GCIs with a specific antibody (16, 126).

In the detergent-insoluble fraction of LBD/PD lysate (containing aggregated forms of αsyn), multiple studies have noted an increase in the truncated αsyn/FL αsyn ratio compared with the soluble fraction and control fractions, suggesting that the presence of certain truncations may be enriched in pathologic inclusions with disease implications (16, 17, 26, 28, 67, 127–129, 131, 132, 134) (Table 1). IHC of pathologic inclusions from synucleinopathy samples using truncation-specific antibodies corroborates the suggested importance of these species. Antibodies specific for αsyn truncated at residues 9, 103, 110, 119, and 122 have been used to detect truncated αsyn within LBs, LNs, and GCIs (16, 128–133), where three studies have stated that the truncated forms of αsyn are more centrally located in these inclusions compared with FL αsyn, suggesting a possible early role for truncated αsyn in the generative processes of these inclusions (124, 128, 130). Regional variation in the amount of truncated αsyn may be important in understanding vulnerability of various loci to early αsyn aggregation if truncated αsyn is linked to initial inclusion formation. Indeed, PD is thought to have early pathologic αsyn formation in the enteric nervous system (98), and it was observed using the appendix from PD patients that levels of truncated αsyn, particularly C-truncated at residue 125, were greatly elevated compared with the SNpc from the same patients and the appendices of controls (134). Another study found elevated levels of 103 C-truncated αsyn in the colon of PD patients (135). Likewise, findings from our laboratory showed that C-terminal truncation may be highly prevalent in the medial temporal lobe in LBD, which is afflicted early in disease, compared with the cingulate cortex (67). Regional variation of truncated forms of αsyn may also have implications for toxicity; for the 1–103 C-truncated αsyn, a specific antibody was able to detect higher amounts of 103 C-truncated αsyn in the SNpc, where extensive cell death is present, compared with the cortex in PD cases (132). Another study using a truncation-specific antibody in PD brains found that a doubly N- and C-truncated form of αsyn was prone to form punctate aggregates in mitochondria that were associated with mitochondrial dysfunction (133). The consequences of truncated αsyn in pathophysiologic processes are more easily studied in preclinical models, which will be further discussed; however, upon examination of post-mortem samples from diseased human tissue, it is evident that truncated forms of αsyn are involved in the formation of toxic αsyn aggregates.

Although not confirmed to be due to truncation, unique histologic features detectable only with antibodies raised against central epitopes of αsyn and not those against the extreme N or C terminus (presumably lost due to truncation) may provide additional evidence that truncated forms of αsyn are involved in disease. Indeed, central αsyn epitope antibodies have been reported by our laboratory and others to prominently detect pathologic forms of αsyn in astrocytes in LBD that are not often detectable with N- or C-terminal antibodies (21, 67, 136–138). Likewise, central αsyn epitope antibodies have been reported to detect high-molecular-weight bands in the insoluble fraction of LBD lysate that are not apparent when using N- or C-terminal antibodies; this may be due to oligomeric or ubiquitinated forms of truncated αsyn (67, 136, 138).

Cumulatively, these studies show that truncated forms of αsyn are present in disease-associated aggregates in synucleinopathies and may have implications for the initiation and progression of disease.

Detection in healthy brains and splice variants

In the soluble fraction of aged control brains that do not have a synucleinopathy, there is quantitatively less truncated αsyn than in insoluble disease fractions (16, 17, 26, 28, 67, 127–129, 131, 132, 134) (Table 1); the only truncation band present in some studies appears to be the C-truncated 12–15 kDa band, particularly 1–119 αsyn, which is typically of lesser intensity than insoluble disease fractions, although a few studies have not found significant differences (16, 17, 26, 27, 62, 124). At least one article states that more 1–119 αsyn is detected in the soluble fraction of diseased brains compared with controls (26), whereas other studies see little to no change (16, 17, 27, 124). Although 1–119 αsyn is found to some degree in the soluble fraction of both diseased and control brains, it is only found to form insoluble pathologic inclusions in disease (16, 130).

Although not necessarily truncated by a protease, there exist at least three splice variants of αsyn that are missing either exon 5 (residues 103–130), exon 3 (residues 41–54), or both, resulting in variants termed αsyn 112, αsyn 126, or αsyn 98 (139). These variants, particularly those missing C-terminal residues through

exon 5 removal, may display properties similar to those of C-truncated αsyn, such as increased aggregation, which will be further discussed (reviewed in Ref. 139). There have been multiple observations that the mRNA ratios of these splice variants relative to FL αsyn are altered in disease, often in a region-specific manner (reviewed in Ref. 139); however, it is difficult to correlate this with resulting changes in αsyn proteoforms due to the low abundance of the variants, and consequently they are not typically observable on a Western blotting or IHC even with a splice variant–specific antibody (26, 124). Additionally, the majority of truncated forms of αsyn isolated from LB extract are consistent with formation from various proteases (discussed below), suggesting that alterations in splicing machinery are not the major source of αsyn variants in disease (41).

Detection in mouse models of disease

In murine models based on overexpression of FL human αsyn (often containing the aggregation-prone A53T mutation), truncated αsyn is similarly observable when insoluble LB-like aggregates form (140). Two studies found that overexpression of human A53T αsyn in mice results in clear truncated αsyn bands of 12, 10, and 8 kDa in size that are enriched in the insoluble fraction in regions containing LB-like pathology, which is similar to the patterns described for human disease (26, 140). These bands are not found in nontransgenic mice (26, 140), as they do not develop insoluble αsyn. Also, it has been found that overexpression of human αsyn in cultured cells results in more αsyn truncation compared with mouse αsyn overexpression (26). A similar pattern was observed with a separate A53T αsyn mouse model, where three truncation bands were observed in the insoluble fraction of sick mice with two bands (~13 and ~10 kDa) being only C-truncated and one (~7–8 kDa) being both N- and C-truncated; these truncation bands were roughly similar to those seen in the insoluble fraction of LBD lysate in the same study (17). A more recent experiment used MS to determine that truncated αsyn in sick A53T human αsyn transgenic mice (same mouse line as the previous study) is mainly the 1–122 form found in humans, but also 1–90 that has not previously been detected in human disease; thus, some differences may be present between mouse models and human disease; lesser amounts of other forms of truncated αsyn were also detected, including 1–103, 1–124, and 5–140, that are prominent in human LBs (141) (Table 1). In a mouse model overexpressing A30P αsyn, punctate inclusions in sick mice were labeled with truncation-specific antibodies but not in non-sick transgenic mice or age-matched nontransgenic controls, further suggesting that the appearance of truncated αsyn is linked to the appearance of pathologic inclusions; other truncations were identified using MS (128). Even in mice overexpressing WT human αsyn, accumulation of C-truncated αsyn at residue 122 was noted upon Western blotting of symptomatic mice that was not present in nontransgenic mice; 122 C-truncated αsyn was also noted to be present in punctate inclusions and dystrophic neurites with similar patterns to LBD samples in the same study (131).

In addition to overexpression models of synucleinopathy, truncation of αsyn appears to be present in prion-like models as well. When nontransgenic mice were intracerebrally injected with PFFs, a truncation-specific antibody was used to detect a doubly N- and C-truncated form of αsyn linked to mitochondrial toxicity in human samples, which was not present in controls (133). From these reviewed studies, it is apparent that truncated αsyn forms in murine models of synucleinopathy in relation to the development of pathologic αsyn inclusions and subsequent symptoms.

Pathologic consequences of αsyn truncation

C-terminal truncation of αsyn increases pathologic aggregation

The C terminus of αsyn harbors multiple protective features to limit pathologic misfolding and aggregation due to several structural factors, and loss of these through truncation promotes fibril formation. First, the C terminus is the most highly charged portion of αsyn due to 15 acidic residues that promote a disordered protein structure and maintain protein solubility (142–144). Events neutralizing the C-terminal charge, such as lowering the pH, binding of cations to residues 119–124, or mutation of the negative residues to neutral or positive ones, promote robust spontaneous aggregation of αsyn into oligomers or fibrils, whereas the addition of extra negative residues decreases fibril formation (36, 142,143, 145–150). Furthermore, the fusion of the C terminus of αsyn to other proteins is sufficient to solubilize them and protect against heat-induced aggregation, demonstrating its anti-aggregative properties (48, 151). Second, the C terminus has autochaperoning abilities, whereby αsyn often adopts conformations in which the C terminus contacts the hydrophobic NAC to shield it from pathologic templating interactions; this behavior is mediated by hydrophobic motifs in residues 115–119 and 125–129 (36, 152–157). When long-range contacts are impaired by the introduction of nanobodies against the C terminus, or the transient interaction with NAC is unfavorable due to high temperature, aggregation is accelerated similar to the impairment of charge (145, 147, 153, 156). In addition, the C terminus is the most proline-rich region in αsyn, with 5 proline residues known to be unfavorable in β-sheet formation; site-directed mutagenesis of these prolines to alanines promotes aggregation (142, 158). All of these protective features are lost upon C-terminal truncation, and consequently C-terminal truncation of αsyn has been repeatedly shown to promote *in vitro* oligomer and fibril formation far more than FL αsyn (17, 22, 26, 29–31, 33–35, 132, 134, 159–164). Comparatively, N-terminal truncation has been shown to either not affect aggregation or mildly decrease it (56, 165, 166), although one study did observe increased aggregation with the removal of N-terminal repeats (167). The lesser effect of N truncation on aggregation is expected due to the comparatively inconsequential changes in basic biochemical properties, such as pI and hydrophobicity, that are induced when the amphipathic N terminus is truncated (22, 165).

In studying how C-terminal truncation affects aggregation *in vitro*, most studies first generate truncated αsyn through purification of recombinant truncated αsyn or through incubation with common cellular proteases. Experimentation to measure aggregation rates usually relies on incubating truncated

monomers of αsyn at physiologic temperatures with shaking and then measuring the rate of amyloid-binding dye fluorescence or biochemical insolubility over time (17, 22, 26, 29–31, 33–35, 132, 134, 159–164). A few studies examined aggregation of truncated forms of αsyn confirmed to exist in LBs (22, 34, 132, 142, 161, 163) or formed from common proteases (132, 134, 160, 162, 164, 168), but most experiments utilized arbitrary C truncations. In general, the *in vitro* studies cumulatively show that the exact site of truncation is not as important as the amount of the C terminus that is lost when assessing aggregation propensity. Removal of only a couple residues, such as with 1–133 and 1–135 αsyn, does not increase the aggregation rate or extent much compared with larger truncation, such as with 1–115 αsyn (22, 29, 31, 34, 142); our laboratory noted that aggregation propensity as measured by both the rate and total extent of aggregation increases rapidly once more than ~10 C-terminal residues are removed (22). Removal of C-terminal αsyn residues somewhat linearly increases aggregation rate and extent up to residues ~85–90, where the NAC domain begins; as NAC residues form the core of the amyloid fibrils, further truncation decreases aggregation (29, 32, 36, 52). C-truncated αsyn may be pathologically relevant not only due to the robust aggregation propensity, but also in synergistically accelerating the aggregation of FL αsyn. Experiments conducted *in vitro* have reported an enhancement of FL αsyn aggregation when co-fibrillized with C-truncated αsyn monomers (17, 22, 26, 29, 132, 160). Indeed, many of these experiments used substoichiometric quantities of truncated αsyn and demonstrated that their presence can induce FL αsyn to aggregate quickly and to a larger extent than would be observed without the truncated αsyn present (22, 26, 29). Moreover, it was demonstrated that this phenomenon can lead to FL αsyn aggregation at substantially lower concentrations, where it would otherwise not occur, close to the physiologic 3 μM cellular concentration of αsyn (13). The extent to which C-truncated αsyn induced FL αsyn to aggregate depended on the extent of truncation, where more heavily truncated 1–115 αsyn induced the most FL αsyn aggregation compared with 1–135 αsyn (22). The mechanism for this synergistic aggregation appears to be co-polymerized C-truncated/FL αsyn fibril formation, as both FL and C-truncated forms of αsyn became insoluble in equal proportions, and both forms are found co-assembled into the same fibrils, as shown with immuno-EM labeling (22).

It is now well-established that C-terminal truncation of αsyn, in line with predicted biochemical changes, greatly increases the tendency of αsyn to misfold into pathologic fibrils. The appearance of even small amounts of C-truncated αsyn may catalyze the misfolding of FL αsyn into fibrils that may initiate the prion-like cycle, as will be discussed.

Truncation of αsyn increases aggregation in cultured cells and murine models

C truncation of αsyn increases aggregation *in vivo* as well; in addition to the structural aspects, removal of the C terminus may further enhance aggregation in a cellular milieu through impaired αsyn degradation due to loss of consensus motifs for ubiquitin ligases and chaperone mediators of autophagy (169–171) and through loss of normally protective C-terminal interactions, such as binding of oxidized dopamine (172, 173). Although not as numerous as the *in vitro* studies, experiments have been conducted demonstrating that C truncation of αsyn promotes aggregation into pathologic inclusions in cultured cells and animal models (22, 132, 159, 174–183). These same studies often demonstrated toxic consequences from C truncation of αsyn that will be discussed further.

In cultured cells, C-truncated αsyn can spontaneously aggregate more readily than FL αsyn and is more amenable to misfolding induced by PFFs. In stably transfected astrocytoma cells, it was demonstrated that 1–111 αsyn formed more inclusions than FL αsyn–containing cells and additionally, the 1–111 αsyn cells formed higher-molecular weight species detectable on WB that may be oligomers not seen with FL αsyn (177, 178). Likewise, overexpressions of 1–120, 1–108, and 1–103 αsyn have been demonstrated to form more and/or larger inclusions than FL αsyn in cultured cells, including with unique inclusion morphology, as 1–120 αsyn formed larger-volume inclusions than FL αsyn in primary neurons (132, 175, 183). In a prion-like induction cell model, our group studied eight C-truncated forms of both human and mouse αsyn overexpressed in HEK293T cells and demonstrated that with increasing extent of C truncation, there is more aggregation compared with FL αsyn when exposed to the same PFFs as measured by amount of insoluble αsyn formed and number of inclusions observed (22, 159).

Overexpression through viral transduction or transgenesis of certain C-truncated forms of αsyn in *Drosophila* and in murine models have demonstrated that these truncations tend to aggregate into pathologic inclusions more than the FL protein, with additional toxic consequences (132, 174, 179–182, 184–186). Transgenesis with 1–120 αsyn has been the most widely used mouse model for truncated αsyn, as three different lines using different promoters (CamKII-α or rat TH) have demonstrated pathologic inclusion formation in disease-relevant regions, such as the SNpc, striatum, cortex, and olfactory bulb (174, 179, 181). In *Drosophila* overexpressing either FL or 1–120 αsyn, it was noted that 1–120 αsyn resulted in more inclusions and proteinase K–resistant αsyn (180). Adeno-associated virus transduction of either 1–103 or FL αsyn into the SNpc of nontransgenic mice demonstrated that the 1–103 αsyn resulted in more inclusions and dopaminergic cell death (132). Additionally, 1–130, 1–119, or 1–93 αsyn–overexpressing animals were created that did not show evidence of inclusion formation but did all have various pathologies and dopaminergic deficits (184–186).

The tendency of C-truncated αsyn to readily aggregate into pathologic inclusions has been studied *in vivo*, but additionally the synergistic aggregation with FL αsyn observed *in vitro* also occurs in cellular and animal models. Our group demonstrated in HEK293T cells that co-expression of FL αsyn with increasingly C-truncated αsyn leads to a greater proportion of aggregated, insoluble FL αsyn with the presence of more extensive C truncation (22). Likewise, two animal models demonstrated increased αsyn inclusion formation when both FL αsyn and one of 1–110 or 1–120 αsyn were present, which was more than additive (181, 182). These results further demonstrate that

αsyn C truncations may assist in initiating FL αsyn fibrillization. Cumulatively, the *in vitro*, cell culture, and animal experiments reveal that C-truncated αsyn is primed to aggregate, which may be crucial in initial disease pathogenesis.

Fibrils containing truncated αsyn have distinct structures and biochemical properties

Both N and C truncation of monomeric or fibrillar αsyn may result in eventual pathologic fibrils with unique structural and biochemical features, as measured through a battery of assays, including CD, EM, protease digestion and accessibility, and others that will be discussed. Differences in these properties may be suggestive of differing conformations and strains, with resulting alterations in prion-like properties.

As expected from removing a highly acidic region, C truncation of αsyn alters biochemical properties, including increased pI and hydrophobicity (22); for N truncation, the trend is reversed, and increased hydrophilicity and net electrostatic charge is observed (165). CD analysis of C-truncated (29, 31, 36, 187, 188) and N-truncated (167) forms of αsyn mostly demonstrate the typical random coil spectra of FL αsyn (6). One study did note that incubation of monomeric FL αsyn with a protease implicated in ~10–122 αsyn formation, calpain I, resulted in increased β-sheet structure (128). When placed in solvent that promotes structure formation, FL αsyn became partially α-helical, which is physiologic (167); however, N-truncated forms (167) and C-truncated forms (187) became more structured with altered spectra (167, 187, 188), which has been interpreted as the possible formation of misfolded intermediates that may be oligomer-prone (147, 188).

When fibrils were produced from monomers of truncated αsyn *in vitro*, immediate structural differences were noted compared with FL αsyn fibrils. For C truncation, CD analysis and similar techniques indicate a higher percentage of β-sheet structure than FL αsyn fibrils in most studies (29, 31, 56) (although one study detected a decreased percentage (160)), and amyloid-binding dyes may have altered affinity for C-truncated fibrils, indicating an alternative fibril structure (29, 60, 160, 163, 189). The nature of β-sheets within the fibril core of C-truncated αsyn fibrils may be fundamentally different from that of FL αsyn, as one study found evidence that β-sheets are highly "twisted" in C-truncated fibrils (33). Biochemically, C-truncated fibrils have demonstrated altered protease digestion patterns compared with FL αsyn fibrils, which again could imply variable epitope exposure through unique fibril conformations (22, 161, 189).

When studied with EM and atomic force microscopy, most studies find that C-truncated fibrils are unbranched and typical amyloid in appearance with some differences from FL αsyn fibrils (22, 29–31, 33, 35, 36, 56, 60, 132, 160, 161, 189). Fibril width is decreased after C truncation of ~20 residues, which is consistent with the theory that the unstructured C terminus "hangs" off the fibril core (22, 29, 33, 56, 60). These fibrils also tend to be shorter longitudinally, likely due to the increased aggregation rate (22, 31, 35, 189), and have denser lateral packing between fibrils, which may be due to less C-terminal charge (22, 31, 35, 36, 60, 189). Other morphologic properties of C-truncated fibrils observed with EM and other techniques include the formation of "ribbon-like" fibrils (31) and increased "twisting" of paired protofilaments within the fibril compared with FL αsyn (33). The increased twisting in particular may be a key difference, as recent characterization of C-truncated and FL αsyn fibrils through the use of cryo-EM shows that the protofilaments in the truncated fibrils do have a higher helical periodicity compared with FL αsyn, and the increased periodicity is more extreme with more extensive C truncation (58, 161, 190, 191). This increase in twisting upon C truncation is attributed to less steric hindrance between αsyn subunits in the fibril core as the unstructured C termini are removed, leading to tighter packing and increased twisting, resulting in a fundamentally different fibril structure (33, 161).

Comparatively, fibrils comprised of increasingly N-truncated αsyn had less β-strand structure than FL αsyn fibrils in one study (165) but more in two others (56, 167) and also altered amyloid dye binding (189). Upon EM and atomic force microscopy examination, the N-truncated αsyn formed typical amyloid fibrils (56, 167, 189); however, N truncation also decreases the fibril width, as part of the N terminus is not incorporated into the fibril core (56, 167), and in contrast to C-truncated fibrils are longitudinally longer (189). Additionally, protease digestion patterns suggested that N truncation harbors a different fragmentation pattern compared with FL or C-truncated αsyn (189). These results suggest that unique fibril structures may be present for N-truncated αsyn; however, far fewer experiments have been conducted relative to C truncation, and the results are less clear and require further study.

Although experiments utilizing C-truncated αsyn fibrils produced from recombinant C-truncated αsyn are useful, it has been suggested that more physiologically relevant information may be gathered from studying fibril structures incubated with proteases, as this likely results in a mix of N- and C-truncated and FL αsyn in the same fibril. Many of the same structural alterations seen with recombinant C-truncated fibrils are observed on FL αsyn fibrils exposed to common proteases, including a fibril width reduction (32, 39, 56) and an increase in fibril twisting (141). One study noted that a unique single-protofilament fibril structure observed only with recombinant doubly N- and C-truncated αsyn was able to be generated by protease digestion of a FL αsyn fibril, suggesting that truncated fibrils produced through use of recombinant protein may be similar to those produced through proteolysis (56). It seems paradoxical that cleavage of the extreme N and C terminus of αsyn would fundamentally alter the fibril structure, as they are thought to be largely unstructured in fibrils (58); however, the cumulative evidence suggests that C truncation in particular can induce important structural changes with consequences for prion-like seeding, as will be discussed.

Fibrils containing truncated αsyn may alter prion-like seeding of pathology in vitro

The effect of αsyn truncation is important to understand in relation to prion-like seeding, as αsyn fibrils in healthy neurons are quickly trafficked for lysosomal processing, where extensive truncation of exposed N- and C-terminal regions can readily

occur (20, 41, 141, 192). Additionally, C-truncated αsyn may have outsized importance in initial disease regions as discussed previously, and reducing prion-like activity at this stage may be key to disease prevention. The presence of truncated αsyn in fibrils can alter fibril structure and thus theoretically affect prion-like seeding in a strain-like manner. Unlike aggregation properties, the exact truncation site may be important in prion-like seeding analogous to the differing templating properties of Aβ 40 and Aβ 42 (193) or the species barrier in prion phenomena (120), where even a slight difference in the amino acid sequence can have drastic consequences for pathologic propagation.

The ability of truncated αsyn-containing fibrils to induce prion-like conformational templating has been studied in multiple experimental paradigms by producing PFFs containing truncated αsyn (using either recombinant protein or incubation with proteases) and then measuring the formation of αsyn fibrils when added to an *in vitro* solution of physiologic FL αsyn, cultured cells expressing αsyn, or mouse models harboring endogenous αsyn. Although seemingly straightforward, *in vitro* studies have produced mixed results, with some observing increased templating ability (132, 141, 161, 189) of FL αsyn by truncated fibrils and others observing a decrease (32, 33, 163) compared with FL αsyn fibrils. Three of the studies that observed increased templating activity with truncated fibrils used either the fibrils comprised of 1–103 αsyn or fibrils digested by the protease implicated in formation of 1–103 αsyn, AEP (132, 141, 161). Furthermore, it was demonstrated that the 1–103 αsyn fibrils or AEP-cleaved fibrils can propagate their unique twisted fibril morphology onto FL αsyn, demonstrating what could be construed as true prion-like strain behavior (141, 161). The only other truncated αsyn fibrils to show increased seeding activity were comprised of 1–120 αsyn, where FL αsyn was rapidly assembled into fibrils in the presence of the 1–120 αsyn fibrils; furthermore, the resulting templated fibrils again had a unique twisted morphology imparted onto them that was not seen when seeded with FL αsyn fibrils (189). All other examined truncated αsyn fibrils displayed reduced seeding activity of FL αsyn compared with FL αsyn seeds, including fibrils comprised of 1–130 αsyn, 1–110 αsyn, 1–108 αsyn, 1–119 αsyn, 10–140 αsyn, 30–140 αsyn, and calpain I–cleaved αsyn fibrils that were characterized to contain 1–114 and 1–122 αsyn (32, 33, 163); 21–140 αsyn fibrils had similar seeding activity to FL fibrils (189), and a separate study using 1–103 αsyn fibrils observed decreased seeding in contrast to the other 1–103 αsyn studies (163). These results show little trend regarding extent or exact site of truncation, suggesting that prion-like activity of fibrils comprised of each form of truncated αsyn may differ.

The heterogeneous outcomes of the *in vitro* seeding studies with truncated fibrils may be somewhat understood in the context of homotypic seeding. Homotypic seeding is the theory that there must exist structural compatibility between the seeding fibril and templated monomeric protein; this is usually applied to understanding the species barrier in prion propagation, where even one amino acid difference can greatly impair the addition of monomers to the seed fibril (120). One study noted improved seeding capacity of the truncated fibril when added to monomeric αsyn harboring the same truncation (33). Indeed, although 1–108 αsyn fibrils seeded FL αsyn poorly, they promptly templated 1–108 αsyn monomers to elongate the seed fibril (33). This may be a simplistic explanation, as it has also been observed that FL αsyn fibrils may seed C-truncated αsyn monomers equally or superiorly to FL αsyn monomers (22, 33, 159, 163), as the increased aggregation propensity of C-truncated αsyn must also be taken into account, but the general idea of compatibility between seeding fibril and templated monomer is likely occurring to a degree.

It has been proposed that the highly twisted structure of C-truncated αsyn fibrils may impair the addition of FL αsyn monomers to elongate the fibril, as there is increased steric hindrance for the added FL αsyn monomer still containing a C terminus; the reverse, where C-truncated αsyn elongates a FL αsyn fibril, would not be a problem (22, 33). It seems likely that the incompatibility between truncated αsyn fibrils and FL αsyn monomers explains the findings for most experiments; however, for certain truncated fibrils, such as those containing 1–103 αsyn and 1–120 αsyn, there may be true prion-like strain propagation to the templated FL αsyn. Overall, no theory adequately explains the current *in vitro* findings for seeding with truncated αsyn fibrils, and prion-like activity of truncated fibrils must be evaluated on a case-by-case basis, depending on the truncation present.

Fibrils containing truncated αsyn have strain-like variation in seeding capacity in cultured cells and murine models

Extending the study of prion-like seeding capacity of truncated αsyn fibrils to cellular and animal models is complicated due to additional extrinsic factors now involved, such as modulation of cellular uptake and spread of fibrils due to truncation (194, 195), trafficking to subcellular compartments (196), and structural changes to the truncated fibril due to additional PTMs; most of these variables have not been studied in relation to truncated αsyn fibrils or even typical αsyn seeding experiments. Nonetheless, cellular (22, 38, 91–93, 103, 120, 159, 189, 197, 198) and animal (135, 159, 189, 199) experiments using fibrils containing truncated αsyn have shown some similar findings to *in vitro* studies.

In cellular and animal models, there are again heterogeneous results, depending on the exact truncation, where most studies observe decreased seeding of FL αsyn when fibrils are comprised entirely of truncated αsyn (22, 103, 120, 159, 189), some see increased seeding of FL αsyn (38, 160, 189), and others observe equal seeding capacity (91–93, 97, 159, 189, 197–199) compared with FL αsyn fibrils. In most of these studies, analyzing the seeding behavior of truncated αsyn fibrils was not the focus, and likewise mostly qualitative results are available. Fibrils comprised of 21–140 αsyn (91, 93, 97, 189, 198, 199), 58–140 αsyn (92), and 1–89 αsyn (92) have been observed to induce FL αsyn aggregation and inclusion formation equally to FL αsyn fibrils, whereas 1–99 αsyn fibrils showed a decrease (120). Despite the *in vitro* findings that 1–120 and 1–103 αsyn fibrils were excellent seeds of FL αsyn, in cellular models, 1–120 αsyn was either equal to or less than FL αsyn fibrils in seeding (91, 92, 103, 189, 198) and likewise for 1–103 αsyn (135).

Examining only studies that explicitly set out to study the seeding behavior of truncated αsyn in cellular or animal models

provides more outcome measures and discernible trends (22, 38, 159, 160, 189). The only four truncated forms of αsyn to demonstrate increased seeding of FL αsyn as measured by inclusion counts or insoluble αsyn formation were fibrils comprised of 31–140 and 11–140 αsyn in cells and mice (189), 1–121 αsyn in cells (160), and FL αsyn fibrils cleaved by cathepsin B in cells (38). In one comprehensive study, it was found that removal of 10, 20, or 30 C-terminal residues or 20 N-terminal residues resulted in equal or slightly less seeding of FL αsyn pathology in cultured cells and nontransgenic mice, whereas removal of 10 or 30 N-terminal residues increased seeding in the same models; this was in contrast to the *in vitro* results that predicted lesser seeding for all except 1–120 αsyn (189). In our laboratory we have observed a trend utilizing eight different C truncations (residues 1–135) in both mouse and human αsyn and observed that in general, increasing C truncation leads to lessened seeding of FL αsyn in both cellular and animal models (22, 159). Overall, whereas removal of the C terminus appears to impair cross-seeding of FL αsyn to varying degrees, depending on the exact truncation, there appear to be a few truncations that similarly to *in vitro* results may demonstrate true prion-like strain propagation and overcome structural incompatibility, and particularly N-terminal truncation may lead to a potent increase in seeding capacity for FL αsyn. Additionally, many fibrils comprised of truncated αsyn demonstrating potent seeding *in vitro* failed to produce similar findings in cellular and animal models, suggesting that prion-like properties of these fibrils should be chiefly studied in the more complex cellular environment.

Last, whereas evaluation of the prion-like properties of fibrils fully comprised of truncated αsyn may be of benefit, physiologically it is unlikely that a fibril would become entirely truncated. Our laboratory has demonstrated that fibrils containing both C-truncated and FL αsyn in a 1:1 ratio seed similarly to, or slightly less than, FL αsyn fibrils, suggesting that the extreme structural alterations of fibrils comprised of C-truncated αsyn are attenuated in this configuration (22, 159). Additionally, fibrils comprised of truncated αsyn may interact with other neurodegenerative proteins as well, as a seed containing both 1–103 truncated αsyn and truncated tau was superiorly able to induce αsyn pathology when injected into mice compared with 1–103 or FL αsyn fibrils, which were themselves about equal in prion-like potency (135).

Overall, the strain-like properties of αsyn fibrils containing multiple N and C truncations along with other PTMs as would be expected to occur in disease are not currently known and warrant further investigation based on the discussed findings where alterations in the terminal regions can greatly alter prion-like seeding. Most investigative models of synucleinopathy do not appreciate the impact of PTMs on seeding; however, the results discussed here demonstrate that truncation in particular likely contributes to strain-like variation in prion-like properties underlying variance in disease properties.

Truncation of αsyn may increase cellular toxicity through direct and indirect mechanisms

Truncation of αsyn may worsen certain modalities of toxicity in both monomeric and polymerized forms, including direct toxicity and indirect mechanisms (loss of function due to truncation or potentiation as an inflammatory agent (200)). Particularly, multiple studies have observed either an increase in oxidative stress or inability to handle oxidative stress in cells containing C-truncated, but also N-truncated, αsyn (17, 133, 177, 201). Additionally, animal models overexpressing C-truncated αsyn in dopaminergic cells have invariably found dysfunction to occur that may be secondary to increased oxidative stress (132, 174, 179–182, 184–186, 202).

Dopaminergic cells of the SNpc are particularly prone to oxidative stress due in part to baseline high bioenergetic demands and production of reactive dopamine quinones, and even slight perturbances in reactive oxygen species production through mechanisms such as mitochondrial dysfunction may induce toxicity (203). When overexpressed, C-truncated forms of αsyn appear to be particularly potent in compromising various cell lines in their ability to handle oxidative stress, and the effect is more than that exerted by FL αsyn (17, 160, 177, 201). Cell viability was generally decreased when C-truncated forms were expressed compared with FL αsyn, demonstrating the toxicity of these species (17, 160, 177, 201). Mechanistically, C-truncated αsyn may cause oxidative stress through mitochondrial dysfunction, as a doubly N- and C-truncated protofibrillary form of αsyn has been shown to accumulate in the mitochondria of diseased cells with deleterious consequences for the hosting mitochondria (133); similar findings were observed with 1–93 truncated αsyn (186). These toxic effects may primarily be mediated by C truncation of αsyn even though N truncation can also be present, as N truncation alone has not been demonstrated to be more toxic than FL αsyn (166).

Similar to cell culture findings, overexpression of C-truncated αsyn in animal models is demonstrably toxic, often more so than FL αsyn when comparison is performed. Animal models have displayed motor symptoms, filamentous neuronal inclusion formations, and dopaminergic dysfunction in particular, which may be attributed to the cellular vulnerability to oxidative stress (132, 174, 179–182, 184–186, 202). Indeed, overexpression of multiple forms of C-truncated αsyn, including 1–93, 1–110, 1–119, 1–120, and 1–130, leads to impaired dopaminergic cellular function evidenced by reduced striatal dopamine (179, 181, 184, 185, 202), nigral TH cell death (132, 182, 184, 186), and resultant behavioral deficits in tests of motor and cognitive ability (132, 182, 184, 186).

Although not well-studied, C-truncated αsyn is a potent agonist of TLR4 receptors on immune cells, as one study found increased release of inflammatory cytokines, such as IL-6 and TNFα, with 1–111 αsyn compared with FL αsyn (200). Inflammasome-related enzyme caspase-1 is also known to produce C-truncated 1–121 αsyn, and toxicity from 1–121 αsyn overexpression can itself trigger further caspase-1 activity in a vicious cycle (160, 162). We have previously reviewed (21) the role that potentially truncated αsyn may play in resident neuroinflammatory astrocytes in the brain in synucleinopathies, and αsyn PTMs such as truncation add a new domain of inflammatory mechanisms in synucleinopathies needing further study. C-truncated αsyn is mainly studied due to its remarkable ability to aggregate into pathologic fibrils, but removal of C-terminal residues can also produce cellular dysfunction through

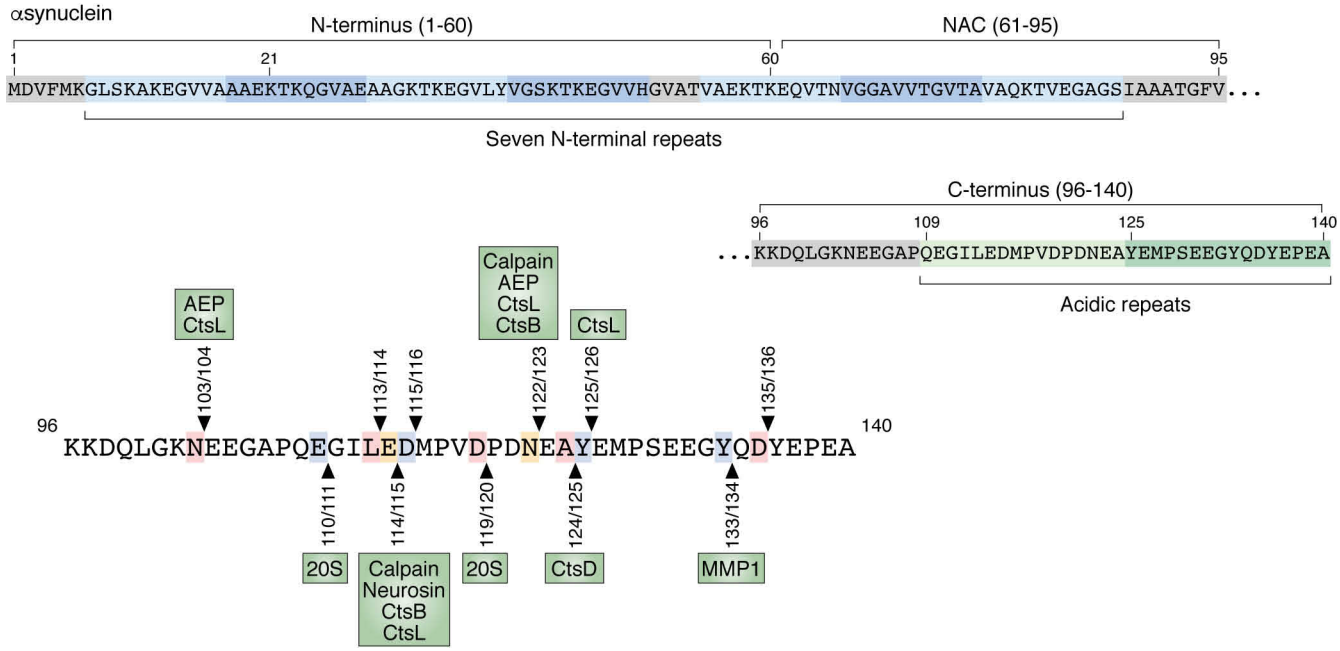

Figure 1. Summary of identified C truncation sites of αsyn in human disease tissue and proteases known to cleave at the indicated αsyn site. All αsyn C truncation sites confirmed with either MS or C truncation–specific antibodies (Table 1) are indicated with *arrows*. Truncations identified were cross-referenced against known cleavage sites in monomeric or fibrillar αsyn for the 20S proteasome (17), cathepsins (Cts) B, D, and L (39, 141), AEP (130, 141), calpain I (32, 40), caspase I (162), neurosin (207), MMP1 to -3 (164), and plasmin (213). The graphic depicting the three domains of αsyn is adapted from Ref. 22. This research was originally published in the Journal of Biological Chemistry. Sorrentino, Z. A., Vijayaraghavan, N., Gorion, K. M., Riffe, C. J., Strang, K. H., Caldwell, J., and Giasson, B. I. Physiological C-terminal truncation of α-synuclein potentiates the prion-like formation of pathological inclusions. *Journal of Biological Chemistry*. 2018; 293:18914–18932. © the American Society for Biochemistry and Molecular Biology.

mitochondrial and oxidative stress, adding another layer of complexity to the pathologic role of truncated αsyn in disease.

Physiologic and pathologic production of truncated αsyn

Endogenous αsyn is chiefly degraded through autophagic pathways (169, 204), whereas pathologic αsyn fibrils are trafficked to lysosomes for sequestration and elimination by cathepsins (20, 39, 41, 141, 192). In both instances, proteases capable of producing truncations relevant to disease act on αsyn, and these proteases are described here and displayed in Fig. 1 along with C-terminal cleavage sites.

Proteases that have been specifically studied in the context of truncating or fully degrading physiologic or misfolded αsyn include the 20S proteasome (17, 26, 205), calpain I (32, 40, 128), caspase I (162), neurosin/kallikrein-6 (206–211), matrix metalloproteases (MMPs) (164, 168, 212), plasmin (213), cathepsins B, D, and L (37–39, 42, 141, 214, 215), and asparagine endopeptidase (AEP) (132, 135, 141, 161). The proteases involved in the production of commonly detected C truncations for both monomeric and fibrillar/oligomeric forms are displayed in Fig. 1. Many of these proteases may be directly linked to disease, as a number have been found co-localized in LB or GCI inclusions (128, 162, 205, 206).

The 20S proteasome may have some activity in degrading cytosolic, soluble αsyn and appears to mainly C-truncate soluble αsyn to the common 1–119 form, with 1–110 and 1–83 also being produced (17, 205). Both 1–119 and 1–110 have been detected in LBs (Table 1); however, the proteasome is not the major producer of 1–119 αsyn, as proteasome blockade does not affect the appearance of the major ~12-kDa C truncation (124) observed in disease lysate (Table 1). Although not considered the major pathway for αsyn clearance, proteasomal dysfunction may have some relevance in synucleinopathies, as monomers of αsyn incubated with 20S proteasome demonstrate increased aggregation (17), proteosomal subunits are detected in LBs (205), and proteosomal activity is diminished in the SNpc in PD (216).

The cytosolic proteases calpain I and caspase I may be an important link between cellular stress and αsyn aggregation as they both predominantly C-truncate αsyn in response to elevated intracellular calcium (calpain I) or inflammasome activation (caspase I). Calpain I has been identified to cleave in both the extreme N terminus and C terminus of fibrillar αsyn and also the NAC region of monomeric αsyn (40); the main truncation stemming from this protease is cleavage after residue 122, although cathepsins may be the main source of the 122 truncation (37, 39). Monomers cleaved by calpain I were observed to readily aggregate in one study (32) but were fully degraded in another (128), which may be due to differences in experimental conditions. Calpain I is co-localized in LBs (32) with cleaved 1–122 αsyn, and its activity is increased in the SNpc of PD patients (217), suggesting a role in disease; additionally, two studies utilizing calpain inhibitors were able to alleviate pathologic findings in mouse models of synucleinopathy (218, 219).

Caspase I is a cytoplasmic protease that is active upon inflammasome assembly, which can be triggered by various deleterious stimuli, such as lipopolysaccharide, cytokines, or other cellular stressors (162). Uniquely, caspase I only appears to

cleave at one site in αsyn, after residue 121. Experiments with 1–121 αsyn have demonstrated rapid assembly into fibrils and potent prion-like seeding with associated toxicity, leading to further inflammasome and capsase I activation, which may cause a pathologic positive feedback cycle in disease (160, 162). Caspase I has been found to co-localize in LBs (162), and administration of a caspase I inhibitor has shown benefit in preserving TH neurons and decreasing αsyn aggregation in a mouse model of MSA (220).

Neurosin, plasmin, and MMPs differ from the other listed proteases in that they are extracellular proteases and thus are unlikely to contribute extensively to intracellular truncated αsyn, although they may truncate extracellular αsyn. Neurosin can cleave within the NAC and C terminus of monomeric and oligomeric αsyn (207–209) and degrade fibrillar αsyn (211) and is mainly thought to be beneficial, as two studies have demonstrated a reduction in αsyn-related pathology when neurosin is overexpressed in mice (209, 210). Neurosin can be found in LBs and GCIs even though it is active only extracellularly, and reduction in its activity is evident in LBD brains (206, 209). Plasmin can truncate monomeric or fibrillar αsyn in mainly N-terminal regions, which for extracellular fibrils decreases their ability to translocate into adjacent cells, thus impacting spreading (213). Of the MMPs, it appears that MMP3 mainly truncates αsyn in the C-terminal region, and fragments produced from MMP3 cleavage of αsyn aggregate more readily into fibrils and protofibrils than FL αsyn and produce more toxicity in cultured cells (164, 168, 186). Incubation of MMP1 with αsyn also results in an increase in aggregation of the fragments through truncation (164), whereas other studied MMPs do not exhibit this effect and sufficiently degrade αsyn (164, 168, 212). The ubiquitous presence of these proteases in the extracellular matrix suggests that αsyn fibrils may undergo some degree of truncation during intercellular spread, and resulting alterations in prion-like activity may result.

The most common proteases in truncating both monomeric and fibrillar αsyn are lysosomal proteases, where most physiologic and pathologic αsyn is normally degraded (39, 169, 204). Of the lysosomal proteases, AEP and cathepsins B, D, and L have been well-characterized in their truncation of αsyn. AEP and its major αsyn truncation product, 1–103 αsyn, have been demonstrated to be uniquely pathologic in their interaction with αsyn (132, 135, 141, 161). AEP has been shown to become overactive in excitotoxicity and aging (132), and high activity of this protease is detected in PD in the SNpc and cortex (132) and possibly the colon (135), where αsyn pathology may begin. The 1–103 αsyn product of AEP is enriched in the brains (132) and colons (135) of PD patients, and this C-truncated αsyn has been continuously shown to readily aggregate into toxic fibrils that can template further pathology (132, 135, 141, 161).

The lysosomal cathepsins have been characterized as the main proteases involved in normal breakdown of monomeric and fibrillar αsyn (37, 39, 204). In terms of their ability to degrade αsyn, cathepsin D is the least efficient, only being able to C-truncate both monomeric or fibrillar αsyn; cathepsin B is able to degrade monomeric but only truncate fibrillar αsyn, whereas cathepsin L can fully degrade all forms of αsyn (39, 141, 215). Combined action of these cathepsins results in the appearance of many common truncated forms of αsyn identified (Table 1), including C truncation after residues 103 (cathepsin L), 122 (cathepsin B or L), 114 (cathepsin B), and 124 (cathepsin D) (39, 141). Cathepsin D has been observed to be dysregulated in mouse models of synucleinopathy, which can be rectified with overexpression of the antioxidant transcriptional activator Nrf2 (221); likewise, in cultured cells it was demonstrated that oxidative stress induced cathepsin D overactivation and the appearance of oligomeric, truncated αsyn (214). It has been suggested that oxidative stress can shift the balance of proteolytic activity in favor of cathepsin D over cathepsin B or cathepsin L (222), which would in turn lead to an increase in partially degraded, truncated forms of αsyn. Compared with cathepsin D, cathepsin B is not as implicated in the formation of truncated αsyn; however, incubation of FL αsyn fibrils with cathepsin B has been shown to produce truncated αsyn fibrils with increased prion-like seeding that can be prevented with a cathepsin B inhibitor (38).

There is still much work to be done in identifying which proteases are responsible for forming truncated forms of αsyn found thus far in human disease (Table 1) and in human cells treated with pathologic αsyn (41), as many of these truncations do not have a suggested protease implicated in their formation, which is summarized in Fig. 1 Proteases that are, in theory, particularly prone to partial degradation of αsyn into C-truncated forms include the 20S proteasome, calpain I, caspase I, AEP, MMP1 and -3, and cathepsin D and B. Many of these enzymes have been demonstrated to display increased activity in situations of oxidative stress, which in combination with impaired proteostasis is a hallmark of aging, the main risk factor in developing neurodegenerative disease (223). Regional variability in these truncating proteases' activity has been observed (224) and may play a role in initiation and progression of synucleinopathies, particularly in the colon in PD, where the appendix displays extensive proteolysis favoring αsyn truncation, which is not seen in healthy controls. Therapies targeting these proteases have proven somewhat effective in preclinical models, and further understanding of detrimental protease activity in synucleinopathies may uncover efficacious treatment strategies aimed at preventing harmful truncation of αsyn.

Summary and future directions

The main genetic risk factors for PD are centered around lysosomal activity (225), and dysfunction of autophagy and proteostasis in general is taking center stage in understanding why synucleinopathies begin and how they progress (226). Truncation of αsyn has been the focus of this review, and inability of proteostatic mechanisms to fully degrade physiologic or pathologic αsyn is the cause of this PTM. Truncated forms of αsyn are common occurrences in synucleinopathies where a number of major C truncations are often present, including those cleaved after residues 103, 115, 119, 122, 125, 133, and 135 (Table 1). Many of these truncations are enriched within the disease-associated insoluble fraction of brain lysate and not

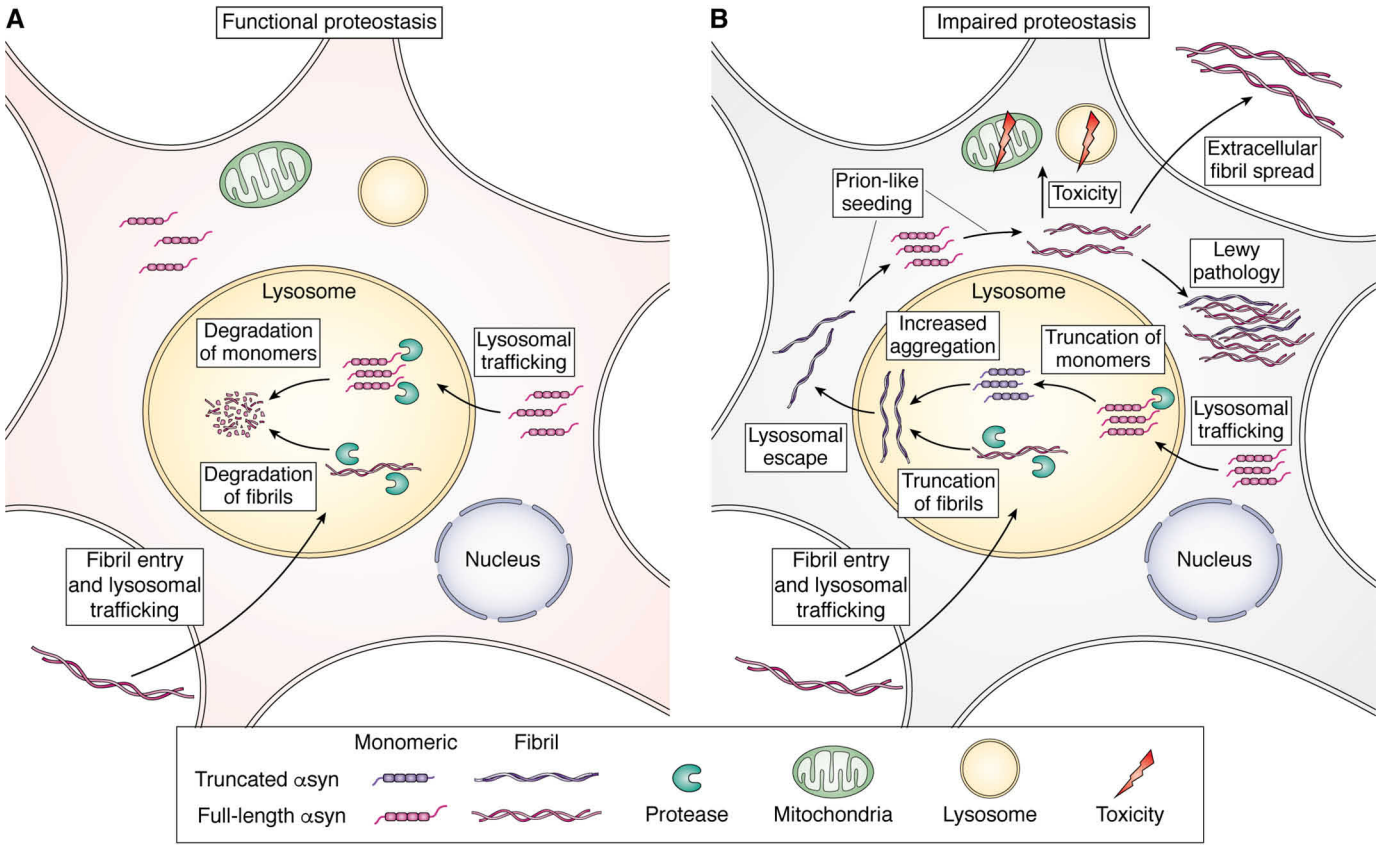

Figure 2. Depiction of pathologic role of αsyn truncation in initiation and propagation of αsyn aggregation. *A*, in healthy neuronal cells, lysosomal enzymes are capable of fully degrading both monomeric and fibrillar forms of αsyn, which prevents both spontaneous formation of aggregates and prion-like seeding from uptaken extracellular fibrils. *B*, in unhealthy neuronal cells, due to cumulative insults including impaired lysosomal autophagy and oxidative stress, only partial degradation of monomeric and fibrillar forms of αsyn occurs. Accumulation of C-truncated monomeric αsyn may kick start initial aggregation and fibril formation, leading to the prion-like seeding cycle of pathology propagation. In continued disease, incomplete degradation of fibrils leads to truncation-containing fibrils with altered prion-like seeding activity. Ultimately, persistence of αsyn aggregates is cytotoxic through various mechanisms, including impairment of autophagy and mitochondrial damage. Image initially created with Biorender.

commonly found in healthy controls, which is indicative of their role in disease pathogenesis but may also prove useful as a peripheral biomarker. Tissue from the regions involved early in PD and LBD, such as the vermiform appendix and amygdala, are rife with truncated forms of αsyn compared with controls (Table 1), and cellular export of these species may signify dysfunctional proteostasis in these vulnerable regions. C truncation of αsyn once formed has the capacity to initiate misfolding and assembly of αsyn into amyloid fibrils, as loss of the C terminus allows the hydrophobic NAC motif to interact with other αsyn proteins to polymerize, which has been demonstrated by a vast repertoire of experimental techniques both *in vitro* and *in vivo*. It is difficult to overstate how rapidly the removal of the C terminus of αsyn allows pathologic aggregation to occur compared with FL αsyn, as removal of even 20 residues results in fibril formation at concentrations that are 4 times less than that required for FL αsyn (31). Once formed, these truncated fibrils may lead to prion-like seeding of endogenous FL αsyn to kick start a vicious cycle in which new fibrils may spread from one cell to the next and propagate therein (Fig. 2). As opposed to aggregation, where increased C-terminal truncation seems to continually increase aggregation up to a point, prion-like properties were heavily dependent on the exact composition of the truncated fibril in terms of N and C truncations present along with possibly other PTMs or even proteins such as tau. Even after FL αsyn fibrils are formed, it is likely that they will come to be truncated as well due to extracellular proteases they are exposed to in intercellular spreading, lysosomal proteases upon endocytic uptake, and cytoplasmic proteases if they manage to escape the lysosome. Indeed, multiple studies have found that FL αsyn fibrils added to cells are quickly trafficked to lysosomes and rapidly truncated (41, 141), which indicates that these truncated αsyn fibrils may be the true prion-like entity that templates endogenous neuronal αsyn and results in toxic sequelae.

Truncated αsyn may theoretically have a role in nearly every stage of αsyn pathologic misfolding and prion-like propagation as we have reviewed, and this should be kept in mind for the design of experiments and therapeutic strategies. As discussed, interventions aiming to preserve proteostatic health and decrease truncated αsyn have shown promise (209, 210, 218–220). Likewise, immunotherapeutic targeting of 122 C-truncated αsyn was beneficial in ameliorating pathologic outcomes in a mouse model of PD, as the presence of this truncation may be highly specific for misfolded αsyn (227). Ultimately, targeting the factors inducing initial misfolding of αsyn, such as truncation and other possible PTMs, or alteration of the cellular milieu, including oxidative or proteostatic stress, in

areas vulnerable to early pathology will be the most efficacious strategy to prevent prion-like propagation and development of symptomatic disease.

Funding and additional information—This work was supported by National Institutes of Health Grants R01NS089022 and R01NS100876 (to B. I. G.) and the University of Florida Moonshot Initiative. Z. A. S. was supported by National Institutes of Health Grant F30AG063446 (to Z. A. S.). The content is solely the responsibility of the authors and does not necessarily represent the official views of the National Institutes of Health.

Conflict of interest—The authors declare that they have no conflicts of interest with the contents of this article.

Abbreviations—The abbreviations used are: AD, Alzheimer's disease; PD, Parkinson's disease; AEP, asparagine endopeptidase; αsyn, α-synuclein; FL, full-length; GCI, glial cytoplasmic inclusion; IHC, immunohistochemistry; ; LB, Lewy body; LBD, Lewy body dementia; LN, Lewy neurite; LRP, Lewy-related pathology; MMP, matrix metalloprotease; MSA, multiple system atrophy; NAC, non-amyloid component; pSer-129, phosphorylated Ser-129 α-synuclein; PTM, post-translational modification; PFF, preformed fibril; SNpc, substantia nigra pars compacta; TH, tyrosine hydroxylase; WB, Western blotting.

References

1. Prince, M., Wimo, A., Guerchet, M., Ali, G.-C., Wu, Y.-T., and Prina, M. (2015) World Alzheimer Report 2015. The Global Impact of Dementia. An Analysis of Prevalence, Incidence, Cost and Trends, Alzheimer's Disease International, London
2. Erkkinen, M. G., Kim, M.-O., and Geschwind, M. D. (2018) Clinical neurology and epidemiology of the major neurodegenerative diseases. *Cold Spring Harb. Perspect. Biol.* **10,** a033118 CrossRef Medline
3. Kovacs, G. G. (2016) Molecular pathological classification of neurodegenerative diseases: turning towards precision medicine. *Int. J. Mol. Sci* **17,** 189 CrossRef Medline
4. Jellinger, K. A. (2012) Interaction between pathogenic proteins in neurodegenerative disorders. *J. Cell. Mol. Med.* **16,** 1166–1183 CrossRef Medline
5. Bendor, J. T., Logan, T. P., and Edwards, R. H. (2013) The function of α-synuclein. *Neuron* **79,** 1044–1066 CrossRef Medline
6. Weinreb, P. H., Zhen, W., Poon, A. W., Conway, K. A., and Lansbury, P. T. (1996) NACP, a protein implicated in Alzheimer's disease and learning, is natively unfolded. *Biochemistry* **35,** 13709–13715 CrossRef Medline
7. Halliday, G. M., Holton, J. L., Revesz, T., and Dickson, D. W. (2011) Neuropathology underlying clinical variability in patients with synucleinopathies. *Acta Neuropathol.* **122,** 187–204 CrossRef Medline
8. Araki, K., Yagi, N., Aoyama, K., Choong, C.-J., Hayakawa, H., Fujimura, H., Nagai, Y., Goto, Y., and Mochizuki, H. (2019) Parkinson's disease is a type of amyloidosis featuring accumulation of amyloid fibrils of α-synuclein. *Proc. Natl. Acad. Sci. U. S. A.* **116,** 17963–17969 CrossRef Medline
9. Spillantini, M. G., Crowther, R. A., Jakes, R., Hasegawa, M., and Goedert, M. (1998) α-Synuclein in filamentous inclusions of Lewy bodies from Parkinson's disease and dementia with Lewy bodies. *Proc. Natl. Acad. Sci. U. S. A.* **95,** 6469–6473 CrossRef Medline
10. Spillantini, M. G., Crowther, R. A., Jakes, R., Cairns, N. J., Lantos, P. L., and Goedert, M. (1998) Filamentous α-synuclein inclusions link multiple system atrophy with Parkinson's disease and dementia with Lewy bodies. *Neurosci. Lett.* **251,** 205–208 CrossRef Medline
11. Bengoa-Vergniory, N., Roberts, R. F., Wade-Martins, R., and Alegre-Abarrategui, J. (2017) α-Synuclein oligomers: a new hope. *Acta Neuropathol.* **134,** 819–838 CrossRef Medline
12. Cremades, N., Cohen, S. I. A., Deas, E., Abramov, A. Y., Chen, A. Y., Orte, A., Sandal, M., Clarke, R. W., Dunne, P., Aprile, F. A., Bertoncini, C. W., Wood, N. W., Knowles, T. P. J., Dobson, C. M., and Klenerman, D. (2012) Direct observation of the interconversion of normal and toxic forms of α-synuclein. *Cell* **149,** 1048–1059 CrossRef Medline
13. Iljina, M., Garcia, G. A., Horrocks, M. H., Tosatto, L., Choi, M. L., Ganzinger, K. A., Abramov, A. Y., Gandhi, S., Wood, N. W., Cremades, N., Dobson, C. M., Knowles, T. P. J., and Klenerman, D. (2016) Kinetic model of the aggregation of α-synuclein provides insights into prion-like spreading. *Proc. Natl. Acad. Sci. U. S. A.* **113,** E1206–E1215 CrossRef Medline
14. Peelaerts, W., Bousset, L., Van der Perren, A., Moskalyuk, A., Pulizzi, R., Giugliano, M., Van den Haute, C., Melki, R., and Baekelandt, V. (2015) α-Synuclein strains cause distinct synucleinopathies after local and systemic administration. *Nature* **522,** 340–344 CrossRef Medline
15. Froula, J. M., Castellana-Cruz, M., Anabtawi, N. M., Camino, J. D., Chen, S. W., Thrasher, D. R., Freire, J., Yazdi, A. A., Fleming, S., Dobson, C. M., Kumita, J. R., Cremades, N., and Volpicelli-Daley, L. A. (2019) Defining α-synuclein species responsible for Parkinson's disease phenotypes in mice. *J. Biol. Chem.* **294,** 10392–10406 CrossRef Medline
16. Anderson, J. P., Walker, D. E., Goldstein, J. M., de Laat, R., Banducci, K., Caccavello, R. J., Barbour, R., Huang, J., Kling, K., Lee, M., Diep, L., Keim, P. S., Shen, X., Chataway, T., Schlossmacher, M. G., *et al.* (2006) Phosphorylation of Ser-129 is the dominant pathological modification of α-synuclein in familial and sporadic Lewy body disease. *J. Biol. Chem.* **281,** 29739–29752 CrossRef Medline
17. Liu, C.-W., Giasson, B. I., Lewis, K. A., Lee, V. M., Demartino, G. N., and Thomas, P. J. (2005) A precipitating role for truncated α-synuclein and the proteasome in α-synuclein aggregation: implications for pathogenesis of Parkinson disease. *J. Biol. Chem.* **280,** 22670–22678 CrossRef Medline
18. Zhang, J., Li, X., and Li, J. D. (2019) The roles of post-translational modifications on α-synuclein in the pathogenesis of Parkinson's diseases. *Front. Neurosci.* **13,** 381 CrossRef Medline
19. Wong, Y. C., and Krainc, D. (2017) α-Synuclein toxicity in neurodegeneration: mechanism and therapeutic strategies. *Nat. Med.* **23,** 1–13 CrossRef Medline
20. Karpowicz, R. J., Trojanowski, J. Q., and Lee, V. M.-Y. (2019) Transmission of α-synuclein seeds in neurodegenerative disease: recent developments. *Lab. Investig.* **99,** 971–981 CrossRef Medline
21. Sorrentino, Z. A., Giasson, B. I., and Chakrabarty, P. (2019) α-Synuclein and astrocytes: tracing the pathways from homeostasis to neurodegeneration in Lewy body disease. *Acta Neuropathol.* **138,** 1–21 CrossRef Medline
22. Sorrentino, Z. A., Vijayaraghavan, N., Gorion, K. M., Riffe, C. J., Strang, K. H., Caldwell, J., and Giasson, B. I. (2018) Physiological C-terminal truncation of α-synuclein potentiates the prion-like formation of pathological inclusions. *J. Biol. Chem.* **293,** 18914–18932 CrossRef Medline
23. Dias, V., Junn, E., and Mouradian, M. M. (2013) The role of oxidative stress in Parkinson's disease. *J. Parkinsons. Dis.* **3,** 461–491 CrossRef Medline
24. Poewe, W., Seppi, K., Tanner, C. M., Halliday, G. M., Brundin, P., Volkmann, J., Schrag, A.-E., and Lang, A. E. (2017) Parkinson disease. *Nat. Rev. Dis. Primers* **3,** 17013 CrossRef Medline
25. Arotcarena, M.-L., Teil, M., and Dehay, B. (2019) Autophagy in synucleinopathy: the overwhelmed and defective machinery. *Cells* **8,** 565 CrossRef Medline
26. Li, W., West, N., Colla, E., Pletnikova, O., Troncoso, J. C., Marsh, L., Dawson, T. M., Jäkälä, P., Hartmann, T., Price, D. L., and Lee, M. K. (2005) Aggregation promoting C-terminal truncation of α-synuclein is a normal cellular process and is enhanced by the familial Parkinson's disease-linked mutations. *Proc. Natl. Acad. Sci. U. S. A.* **102,** 2162–2167 CrossRef Medline
27. Kellie, J. F., Higgs, R. E., Ryder, J. W., Major, A., Beach, T. G., Adler, C. H., Merchant, K., and Knierman, M. D. (2015) Quantitative measurement of intact α-synuclein proteoforms from post-mortem control and

Parkinson's disease brain tissue by intact protein mass spectrometry. *Sci. Rep.* **4,** 5797 CrossRef Medline
28. Baba, M., Nakajo, S., Tu, P. H., Tomita, T., Nakaya, K., Lee, V. M., Trojanowski, J. Q., and Iwatsubo, T. (1998) Aggregation of α-synuclein in Lewy bodies of sporadic Parkinson's disease and dementia with Lewy bodies. *Am. J. Pathol.* **152,** 879–884 Medline
29. Murray, I. V. J., Giasson, B. I., Quinn, S. M., Koppaka, V., Axelsen, P. H., Ischiropoulos, H., Trojanowski, J. Q., and Lee, V. M.-Y. (2003) Role of α-synuclein carboxy-terminus on fibril formation *in vitro*. *Biochemistry* **42,** 8530–8540 CrossRef Medline
30. Crowther, R. A., Jakes, R., Spillantini, M. G., and Goedert, M. (1998) Synthetic filaments assembled from C-terminally truncated α-synuclein. *FEBS Lett.* **436,** 309–312 CrossRef Medline
31. Serpell, L. C., Berriman, J., Jakes, R., Goedert, M., and Crowther, R. A. (2000) Fiber diffraction of synthetic α-synuclein filaments shows amyloid-like cross-β conformation. *Proc. Natl. Acad. Sci. U. S. A.* **97,** 4897–4902 CrossRef Medline
32. Mishizen-Eberz, A. J., Norris, E. H., Giasson, B. I., Hodara, R., Ischiropoulos, H., Lee, V. M.-Y., Trojanowski, J. Q., and Lynch, D. R. (2005) Cleavage of α-synuclein by calpain: potential role in degradation of fibrillized and nitrated species of α-synuclein. *Biochemistry* **44,** 7818–7829 CrossRef Medline
33. Iyer, A., Roeters, S. J., Kogan, V., Woutersen, S., Claessens, M. M. A. E., and Subramaniam, V. (2017) C-terminal truncated α-synuclein fibrils contain strongly twisted β-sheets. *J. Am. Chem. Soc.* **139,** 15392–15400 CrossRef Medline
34. Levitan, K., Chereau, D., Cohen, S. I. A., Knowles, T. P. J., Dobson, C. M., Fink, A. L., Anderson, J. P., Goldstein, J. M., and Millhauser, G. L. (2011) Conserved C-terminal charge exerts a profound influence on the aggregation rate of α-synuclein. *J. Mol. Biol.* **411,** 329–333 CrossRef Medline
35. Hoyer, W., Cherny, D., Subramaniam, V., and Jovin, T. M. (2004) Rapid self-assembly of α-synuclein observed by *in situ* atomic force microscopy. *J. Mol. Biol.* **340,** 127–139 CrossRef Medline
36. Hoyer, W., Cherny, D., Subramaniam, V., and Jovin, T. M. (2004) Impact of the acidic C-terminal region comprising amino acids 109-140 on α-synuclein aggregation *in vitro*. *Biochemistry* **43,** 16233–16242 CrossRef Medline
37. Sevlever, D., Jiang, P., and Yen, S.-H. C. (2008) Cathepsin D is the main lysosomal enzyme involved in the degradation of α-synuclein and generation of its carboxy-terminally truncated species. *Biochemistry* **47,** 9678–9687 CrossRef Medline
38. Tsujimura, A., Taguchi, K., Watanabe, Y., Tatebe, H., Tokuda, T., Mizuno, T., and Tanaka, M. (2015) Lysosomal enzyme cathepsin B enhances the aggregate forming activity of exogenous α-synuclein fibrils. *Neurobiol. Dis.* **73,** 244–253 CrossRef Medline
39. McGlinchey, R. P., and Lee, J. C. (2015) Cysteine cathepsins are essential in lysosomal degradation of α-synuclein. *Proc. Natl. Acad. Sci. U. S. A.* **112,** 9322–9327 CrossRef Medline
40. Mishizen-Eberz, A. J., Guttmann, R. P., Giasson, B. I., Day, G. A., Hodara, R., Ischiropoulos, H., Lee, V. M.-Y., Trojanowski, J. Q., and Lynch, D. R. (2003) Distinct cleavage patterns of normal and pathologic forms of α-synuclein by calpain I *in vitro*. *J. Neurochem.* **86,** 836–847 CrossRef Medline
41. Pieri, L., Chafey, P., Le Gall, M., Clary, G., Melki, R., and Redeker, V. (2016) Cellular response of human neuroblastoma cells to α-synuclein fibrils, the main constituent of Lewy bodies. *Biochim. Biophys. Acta* **1860,** 8–19 CrossRef Medline
42. Hossain, S., Alim, A., Takeda, K., Kaji, H., Shinoda, T., and Uéda, K. (2001) Limited proteolysis of NACP/α-synuclein. *J. Alzheimers. Dis.* **3,** 577–584 CrossRef Medline
43. Kaushik, S., and Cuervo, A. M. (2018) The coming of age of chaperone-mediated autophagy. *Nat. Rev. Mol. Cell Biol.* **19,** 365–381 CrossRef Medline
44. Maroteaux, L., Campanelli, J. T., and Scheller, R. H. (1988) Synuclein: a neuron-specific protein localized to the nucleus and presynaptic nerve terminal. *J. Neurosci.* **8,** 2804–2815 CrossRef Medline
45. Fusco, G., De Simone, A., Gopinath, T., Vostrikov, V., Vendruscolo, M., Dobson, C. M., and Veglia, G. (2014) Direct observation of the three regions in α-synuclein that determine its membrane-bound behaviour. *Nat. Commun.* **5,** 3827 CrossRef Medline
46. Fusco, G., Pape, T., Stephens, A. D., Mahou, P., Costa, A. R., Kaminski, C. F., Kaminski Schierle, G. S., Vendruscolo, M., Veglia, G., Dobson, C. M., and De Simone, A. (2016) Structural basis of synaptic vesicle assembly promoted by α-synuclein. *Nat. Commun.* **7,** 12563 CrossRef Medline
47. Chandra, S., Gallardo, G., Fernández-Chacón, R., Schlüter, O. M., and Südhof, T. C. (2005) α-Synuclein cooperates with CSPα in preventing neurodegeneration. *Cell* **123,** 383–396 CrossRef Medline
48. Park, S. M., Jung, H. Y., Kim, T. D., Park, J. H., Yang, C.-H., and Kim, J. (2002) Distinct roles of the N-terminal-binding domain and the C-terminal-solubilizing domain of α-synuclein, a molecular chaperone. *J. Biol. Chem.* **277,** 28512–28520 CrossRef Medline
49. Souza, J. M., Giasson, B. I., Lee, V. M., and Ischiropoulos, H. (2000) Chaperone-like activity of synucleins. *FEBS Lett.* **474,** 116–119 CrossRef Medline
50. Oikawa, T., Nonaka, T., Terada, M., Tamaoka, A., Hisanaga, S.-I., and Hasegawa, M. (2016) α-Synuclein fibrils exhibit gain of toxic function, promoting Tau aggregation and inhibiting microtubule assembly. *J. Biol. Chem.* **291,** 15046–15056 CrossRef Medline
51. Tuttle, M. D., Comellas, G., Nieuwkoop, A. J., Covell, D. J., Berthold, D. A., Kloepper, K. D., Courtney, J. M., Kim, J. K., Barclay, A. M., Kendall, A., Wan, W., Stubbs, G., Schwieters, C. D., Lee, V. M. Y., George, J. M., *et al.* (2016) Solid-state NMR structure of a pathogenic fibril of full-length human α-synuclein. *Nat. Struct. Mol. Biol.* **23,** 409–415 CrossRef Medline
52. Giasson, B. I., Murray, I. V. J., Trojanowski, J. Q., and Lee, V. M.-Y. (2001) A hydrophobic stretch of 12 amino acid residues in the middle of α-synuclein is essential for filament assembly. *J. Biol. Chem.* **276,** 2380–2386 CrossRef Medline
53. Miake, H., Mizusawa, H., Iwatsubo, T., and Hasegawa, M. (2002) Biochemical characterization of the core structure of α-synuclein filaments. *J. Biol. Chem.* **277,** 19213–19219 CrossRef Medline
54. Vilar, M., Chou, H.-T., Lührs, T., Maji, S. K., Riek-Loher, D., Verel, R., Manning, G., Stahlberg, H., and Riek, R. (2008) The fold of α-synuclein fibrils. *Proc. Natl. Acad. Sci. U. S. A.* **105,** 8637–8642 CrossRef Medline
55. Chen, M., Margittai, M., Chen, J., and Langen, R. (2007) Investigation of α-synuclein fibril structure by site-directed spin labeling. *J. Biol. Chem.* **282,** 24970–24979 CrossRef Medline
56. Qin, Z., Hu, D., Han, S., Dong-Pyo Hong, A., and Fink, A. L. (2007) Role of different regions of α-synuclein in the assembly of fibrils. *Biochemistry* **46,** 133322–133330 CrossRef Medline
57. Heise, H., Hoyer, W., Becker, S., Andronesi, O. C., Riedel, D., and Baldus, M. (2005) Molecular-level secondary structure, polymorphism, and dynamics of full-length α-synuclein fibrils studied by solid-state NMR. *Proc. Natl. Acad. Sci. U. S. A.* **102,** 15871–15876 CrossRef Medline
58. Meade, R. M., Fairlie, D. P., and Mason, J. M. (2019) α-Synuclein structure and Parkinson's disease—lessons and emerging principles. *Mol. Neurodegener.* **14,** 29 CrossRef Medline
59. Li, Y., Zhao, C., Luo, F., Liu, Z., Gui, X., Luo, Z., Zhang, X., Li, D., Liu, C., and Li, X. (2018) Amyloid fibril structure of α-synuclein determined by cryo-electron microscopy. *Cell Res.* **28,** 897–903 CrossRef Medline
60. Sweers, K. K. M., van der Werf, K. O., Bennink, M. L., and Subramaniam, V. (2012) Atomic force microscopy under controlled conditions reveals structure of C-terminal region of α-synuclein in amyloid fibrils. *ACS Nano* **6,** 5952–5960 CrossRef Medline
61. Uéda, K., Fukushima, H., Masliah, E., Xia, Y., Iwai, A., Yoshimoto, M., Otero, D. A., Kondo, J., Ihara, Y., and Saitoh, T. (1993) Molecular cloning of cDNA encoding an unrecognized component of amyloid in Alzheimer disease. *Proc. Natl. Acad. Sci. U. S. A.* **90,** 11282–11286 CrossRef Medline
62. Culvenor, J. G., McLean, C. A., Cutt, S., Campbell, B. C., Maher, F., Jäkälä, P., Hartmann, T., Beyreuther, K., Masters, C. L., and Li, Q. X. (1999) Non-Aβ component of Alzheimer's disease amyloid (NAC) revisited. NAC and α-synuclein are not associated with Aβ amyloid. *Am. J. Pathol.* **155,** 1173–1181 CrossRef Medline
63. Polymeropoulos, M. H., Lavedan, C., Leroy, E., Ide, S. E., Dehejia, A., Dutra, A., Pike, B., Root, H., Rubenstein, J., Boyer, R., Stenroos, E. S.,

Chandrasekharappa, S., Athanassiadou, A., Papapetropoulos, T., Johnson, W. G., *et al.* (1997) Mutation in the α-synuclein gene identified in families with Parkinson's disease. *Science* **276,** 2045–2047 CrossRef Medline
64. Spillantini, M. G., Schmidt, M. L., Lee, V. M.-Y., Trojanowski, J. Q., Jakes, R., and Goedert, M. (1997) α-Synuclein in Lewy bodies. *Nature* **388,** 839–840 CrossRef Medline
65. Goedert, M., Spillantini, M. G., Del Tredici, K., and Braak, H. (2013) 100 years of Lewy pathology. *Nat. Rev. Neurol.* **9,** 13–24 CrossRef Medline
66. McCann, H., Stevens, C. H., Cartwright, H., and Halliday, G. M. (2014) α-Synucleinopathy phenotypes. *Parkinsonism Relat. Disord.* **20,** S62–S67 CrossRef Medline
67. Sorrentino, Z. A., Goodwin, M. S., Riffe, C. J., Dhillon, J.-K. S., Xia, Y., Gorion, K.-M., Vijayaraghavan, N., McFarland, K. N., Golbe, L. I., Yachnis, A. T., and Giasson, B. I. (2019) Unique α-synuclein pathology within the amygdala in Lewy body dementia: implications for disease initiation and progression. *Acta Neuropathol. Commun.* **7,** 142 CrossRef Medline
68. Kim, W. S., Kågedal, K., and Halliday, G. M. (2014) α-Synuclein biology in Lewy body diseases. *Alzheimers. Res. Ther.* **6,** 73 CrossRef Medline
69. Tu, P. H., Galvin, J. E., Baba, M., Giasson, B., Tomita, T., Leight, S., Nakajo, S., Iwatsubo, T., Trojanowski, J. Q., and Lee, V. M. (1998) Glial cytoplasmic inclusions in white matter oligodendrocytes of multiple system atrophy brains contain insoluble alpha-synuclein. *Ann. Neurol.* **44,** 415–422 CrossRef Medline
70. Peelaerts, W., Bousset, L., Baekelandt, V., and Melki, R. (2018) α-Synuclein strains and seeding in Parkinson's disease, incidental Lewy body disease, dementia with Lewy bodies and multiple system atrophy: similarities and differences. *Cell Tissue Res.* **373,** 195–212 CrossRef Medline
71. Braak, H., Del Tredici, K., Rüb, U., de Vos, R. A. I., Jansen Steur, E. N. H., and Braak, E. (2003) Staging of brain pathology related to sporadic Parkinson's disease. *Neurobiol. Aging* **24,** 197–211 CrossRef Medline
72. Kalia, L. V., and Lang, A. E. (2015) Parkinson's disease. *Lancet* **386,** 896–912 CrossRef Medline
73. Deng, H., Wang, P., and Jankovic, J. (2018) The genetics of Parkinson disease. *Ageing Res. Rev.* **42,** 72–85 CrossRef Medline
74. Rosborough, K., Patel, N., and Kalia, L. V. (2017) α-Synuclein and parkinsonism: updates and future perspectives. *Curr. Neurol. Neurosci. Rep.* **17,** 31 CrossRef Medline
75. Yoshino, H., Hirano, M., Stoessl, A. J., Imamichi, Y., Ikeda, A., Li, Y., Funayama, M., Yamada, I., Nakamura, Y., Sossi, V., Farrer, M. J., Nishioka, K., and Hattori, N. (2017) Homozygous α-synuclein p.A53V in familial Parkinson's disease. *Neurobiol. Aging* **57,** 248.e7–248.e12 CrossRef Medline
76. Sahay, S., Ghosh, D., Singh, P. K., and Maji, S. K. (2017) Alteration of structure and aggregation of α-synuclein by familial Parkinson's disease associated mutations. *Curr. Protein Pept. Sci.* **18,** 656–676 CrossRef Medline
77. Giasson, B. I., Duda, J. E., Quinn, S. M., Zhang, B., Trojanowski, J. Q., and Lee, V. M.-Y. (2002) Neuronal α-synucleinopathy with severe movement disorder in mice expressing A53T human α-synuclein. *Neuron* **34,** 521–533 CrossRef Medline
78. Koprich, J. B., Kalia, L. V., and Brotchie, J. M. (2017) Animal models of α-synucleinopathy for Parkinson disease drug development. *Nat. Rev. Neurosci.* **18,** 515–529 CrossRef Medline
79. Chartier, S., and Duyckaerts, C. (2018) Is Lewy pathology in the human nervous system chiefly an indicator of neuronal protection or of toxicity? *Cell Tissue Res.* **373,** 149–160 CrossRef Medline
80. Villar-Piqué, A., Lopes da Fonseca, T., and Outeiro, T. F. (2016) Structure, function and toxicity of α-synuclein: the Bermuda triangle in synucleinopathies. *J. Neurochem.* **139,** 240–255 CrossRef Medline
81. Lim, S., Chun, Y., Lee, J. S., and Lee, S.-J. (2016) Neuroinflammation in synucleinopathies. *Brain Pathol.* **26,** 404–409 CrossRef Medline
82. Refolo, V., and Stefanova, N. (2019) Neuroinflammation and glial phenotypic changes in α-synucleinopathies. *Front. Cell. Neurosci.* **13,** 263 CrossRef Medline
83. Uchihara, T., and Giasson, B. I. (2016) Propagation of α-synuclein pathology: hypotheses, discoveries, and yet unresolved questions from experimental and human brain studies. *Acta Neuropathol.* **131,** 49–73 CrossRef Medline
84. Brundin, P., and Melki, R. (2017) Prying into the prion hypothesis for Parkinson's disease. *J. Neurosci.* **37,** 9808–9818 CrossRef Medline
85. Kordower, J. H., Chu, Y., Hauser, R. A., Freeman, T. B., and Olanow, C. W. (2008) Lewy body-like pathology in long-term embryonic nigral transplants in Parkinson's disease. *Nat. Med.* **14,** 504–506 CrossRef Medline
86. Han, H., Weinreb, P. H., and Lansbury, P. T. (1995) The core Alzheimer's peptide NAC forms amyloid fibrils which seed and are seeded by β-amyloid: is NAC a common trigger or target in neurodegenerative disease? *Chem. Biol.* **2,** 163–169 CrossRef
87. Buell, A. K., Galvagnion, C., Gaspar, R., Sparr, E., Vendruscolo, M., Knowles, T. P. J., Linse, S., and Dobson, C. M. (2014) Solution conditions determine the relative importance of nucleation and growth processes in α-synuclein aggregation. *Proc. Natl. Acad. Sci. U. S. A.* **111,** 7671–7676 CrossRef Medline
88. Pinotsi, D., Buell, A. K., Galvagnion, C., Dobson, C. M., Kaminski Schierle, G. S., and Kaminski, C. F. (2014) Direct observation of heterogeneous amyloid fibril growth kinetics via two-color super-resolution microscopy. *Nano Lett.* **14,** 339–345 CrossRef Medline
89. Jung, B. C., Lim, Y.-J., Bae, E.-J., Lee, J. S., Choi, M. S., Lee, M. K., Lee, H.-J., Kim, Y. S., and Lee, S.-J. (2017) Amplification of distinct α-synuclein fibril conformers through protein misfolding cyclic amplification. *Exp. Mol. Med.* **49,** e314 CrossRef Medline
90. Nonaka, T., Watanabe, S. T., Iwatsubo, T., and Hasegawa, M. (2010) Seeded aggregation and toxicity of α-synuclein and Tau. *J. Biol. Chem.* **285,** 34885–34898 CrossRef Medline
91. Waxman, E. A., and Giasson, B. I. (2010) A novel, high-efficiency cellular model of fibrillar α-synuclein inclusions and the examination of mutations that inhibit amyloid formation. *J. Neurochem.* **113,** 374–388 CrossRef Medline
92. Volpicelli-Daley, L. A., Luk, K. C., Patel, T. P., Tanik, S. A., Riddle, D. M., Stieber, A., Meaney, D. F., Trojanowski, J. Q., and Lee, V. M.-Y. (2011) Exogenous α-synuclein fibrils induce Lewy body pathology leading to synaptic dysfunction and neuron death. *Neuron* **72,** 57–71 CrossRef Medline
93. Sacino, A. N., Thomas, M. A., Ceballos-Diaz, C., Cruz, P. E., Rosario, A. M., Lewis, J., Giasson, B. I., and Golde, T. E. (2013) Conformational templating of α-synuclein aggregates in neuronal-glial cultures. *Mol. Neurodegener.* **8,** 17 CrossRef Medline
94. Desplats, P., Lee, H.-J., Bae, E.-J., Patrick, C., Rockenstein, E., Crews, L., Spencer, B., Masliah, E., and Lee, S.-J. (2009) Inclusion formation and neuronal cell death through neuron-to-neuron transmission of α-synuclein. *Proc. Natl. Acad. Sci. U. S. A.* **106,** 13010–13015 CrossRef Medline
95. Luk, K. C., Kehm, V. M., Zhang, B., O'Brien, P., Trojanowski, J. Q., and Lee, V. M. Y. (2012) Intracerebral inoculation of pathological α-synuclein initiates a rapidly progressive neurodegenerative α-synucleinopathy in mice. *J. Exp. Med.* **209,** 975–986 CrossRef Medline
96. Luk, K. C., Kehm, V., Carroll, J., Zhang, B., O'Brien, P., Trojanowski, J. Q., and Lee, V. M.-Y. (2012) Pathological α-synuclein transmission initiates Parkinson-like neurodegeneration in nontransgenic mice. *Science* **338,** 949–953 CrossRef Medline
97. Sacino, A. N., Brooks, M., Thomas, M. A., McKinney, A. B., Lee, S., Regenhardt, R. W., McGarvey, N. H., Ayers, J. I., Notterpek, L., Borchelt, D. R., Golde, T. E., and Giasson, B. I. (2014) Intramuscular injection of α-synuclein induces CNS α-synuclein pathology and a rapid-onset motor phenotype in transgenic mice. *Proc. Natl. Acad. Sci. U. S. A.* **111,** 10732–10737 CrossRef Medline
98. Kim, S., Kwon, S.-H., Kam, T.-I., Panicker, N., Karuppagounder, S. S., Lee, S., Lee, J. H., Kim, W. R., Kook, M., Foss, C. A., Shen, C., Lee, H., Kulkarni, S., Pasricha, P. J., Lee, G., *et al.* (2019) Transneuronal propagation of pathologic α-synuclein from the gut to the brain models Parkinson's disease. *Neuron* **103,** 627–641 CrossRef Medline
99. Del Tredici, K., and Braak, H. (2016) Review: Sporadic Parkinson's disease: development and distribution of α-synuclein pathology. *Neuropathol. Appl. Neurobiol.* **42,** 33–50 CrossRef Medline

100. Rietdijk, C. D., Perez-Pardo, P., Garssen, J., van Wezel, R. J. A., and Kraneveld, A. D. (2017) Exploring Braak's hypothesis of Parkinson's disease. *Front. Neurol.* **8,** 37 CrossRef Medline
101. Bousset, L., Pieri, L., Ruiz-Arlandis, G., Gath, J., Jensen, P. H., Habenstein, B., Madiona, K., Olieric, V., Böckmann, A., Meier, B. H., and Melki, R. (2013) Structural and functional characterization of two α-synuclein strains. *Nat. Commun.* **4,** 2575 CrossRef Medline
102. Gath, J., Bousset, L., Habenstein, B., Melki, R., Böckmann, A., and Meier, B. H. (2014) Unlike twins: an NMR comparison of two α-synuclein polymorphs featuring different toxicity. *PLoS ONE* **9,** e90659 CrossRef Medline
103. Guo, J. L., Covell, D. J., Daniels, J. P., Iba, M., Stieber, A., Zhang, B., Riddle, D. M., Kwong, L. K., Xu, Y., Trojanowski, J. Q., and Lee, V. M. Y. (2013) Distinct α-synuclein strains differentially promote tau inclusions in neurons. *Cell* **154,** 103–117 CrossRef Medline
104. Strohäker, T., Jung, B. C., Liou, S. H., Fernandez, C. O., Riedel, D., Becker, S., Halliday, G. M., Bennati, M., Kim, W. S., Lee, S. J., and Zweckstetter, M. (2019) Structural heterogeneity of α-synuclein fibrils amplified from patient brain extracts. *Nat. Commun.* **10,** 5535 CrossRef Medline
105. Lau, A., So, R. W. L., Lau, H. H. C., Sang, J. C., Ruiz-Riquelme, A., Fleck, S. C., Stuart, E., Menon, S., Visanji, N. P., Meisl, G., Faidi, R., Marano, M. M., Schmitt-Ulms, C., Wang, Z., Fraser, P. E., *et al.* (2020) α-Synuclein strains target distinct brain regions and cell types. *Nat. Neurosci.* **23,** 21–31 CrossRef Medline
106. Peng, C., Gathagan, R. J., Covell, D. J., Medellin, C., Stieber, A., Robinson, J. L., Zhang, B., Pitkin, R. M., Olufemi, M. F., Luk, K. C., Trojanowski, J. Q., and Lee, V. M.-Y. (2018) Cellular milieu imparts distinct pathological α-synuclein strains in α-synucleinopathies. *Nature* **557,** 558–563 CrossRef Medline
107. Campbell, B. C. V., McLean, C. A., Culvenor, J. G., Gai, W. P., Blumbergs, P. C., Jäkälä, P., Beyreuther, K., Masters, C. L., and Li, Q.-X. (2001) The solubility of α-synuclein in multiple system atrophy differs from that of dementia with Lewy bodies and Parkinson's disease. *J. Neurochem.* **76,** 87–96 CrossRef Medline
108. Klingstedt, T., Ghetti, B., Holton, J. L., Ling, H., Nilsson, K. P. R., and Goedert, M. (2019) Luminescent conjugated oligothiophenes distinguish between α-synuclein assemblies of Parkinson's disease and multiple system atrophy. *Acta Neuropathol. Commun.* **7,** 193 CrossRef Medline
109. Uchihara, T., Nakamura, A., Mochizuki, Y., Hayashi, M., Orimo, S., Isozaki, E., and Mizutani, T. (2005) Silver stainings distinguish Lewy bodies and glial cytoplasmic inclusions: comparison between Gallyas-Braak and Campbell-Switzer methods. *Acta Neuropathol.* **110,** 255–260 CrossRef Medline
110. Prusiner, S. B., Woerman, A. L., Mordes, D. A., Watts, J. C., Rampersaud, R., Berry, D. B., Patel, S., Oehler, A., Lowe, J. K., Kravitz, S. N., Geschwind, D. H., Glidden, D. V., Halliday, G. M., Middleton, L. T., Gentleman, S. M., *et al.* (2015) Evidence for α-synuclein prions causing multiple system atrophy in humans with parkinsonism. *Proc. Natl. Acad. Sci. U. S. A.* **112,** E5308–E5317 CrossRef Medline
111. Lavenir, I., Passarella, D., Masuda-Suzukake, M., Curry, A., Holton, J. L., Ghetti, B., and Goedert, M. (2019) Silver staining (Campbell-Switzer) of neuronal α-synuclein assemblies induced by multiple system atrophy and Parkinson's disease brain extracts in transgenic mice. *Acta Neuropathol. Commun.* **7,** 148 CrossRef Medline
112. Woerman, A. L., Watts, J. C., Aoyagi, A., Giles, K., Middleton, L. T., and Prusiner, S. B. (2018) α-synuclein: multiple system atrophy prions. *Cold Spring Harb. Perspect. Med.* **8,** a024588 CrossRef Medline
113. Yamasaki, T. R., Holmes, B. B., Furman, J. L., Dhavale, D. D., Su, B. W., Song, E.-S., Cairns, N. J., Kotzbauer, P. T., and Diamond, M. I. (2019) Parkinson's disease and multiple system atrophy have distinct α-synuclein seed characteristics. *J. Biol. Chem.* **294,** 1045–1058 CrossRef Medline
114. Woerman, A. L., Oehler, A., Kazmi, S. A., Lee, J., Halliday, G. M., Middleton, L. T., Gentleman, S. M., Mordes, D. A., Spina, S., Grinberg, L. T., Olson, S. H., and Prusiner, S. B. (2019) Multiple system atrophy prions retain strain specificity after serial propagation in two different Tg (SNCA*A53T) mouse lines. *Acta Neuropathol.* **137,** 437–454 CrossRef Medline
115. Rutherford, N. J., Dhillon, J.-K. S., Riffe, C. J., Howard, J. K., Brooks, M., and Giasson, B. I. (2017) Comparison of the *in vivo* induction and transmission of α-synuclein pathology by mutant α-synuclein fibril seeds in transgenic mice. *Hum. Mol. Genet.* **26,** 4906–4915 CrossRef Medline
116. Ayers, J. I., Riffe, C. J., Sorrentino, Z. A., Diamond, J., Fagerli, E., Brooks, M., Galaleldeen, A., Hart, P. J., and Giasson, B. I. (2018) Localized induction of wild-type and mutant α-synuclein aggregation reveals propagation along neuroanatomical tracts. *J. Virol.* **92,** e00586-18 CrossRef Medline
117. Hayakawa, H., Nakatani, R., Ikenaka, K., Aguirre, C., Choong, C., Tsuda, H., Nagano, S., Koike, M., Ikeuchi, T., Hasegawa, M., Papa, S. M., Nagai, Y., Mochizuki, H., and Baba, K. (2020) Structurally distinct α-synuclein fibrils induce robust parkinsonian pathology. *Mov. Disord.* **35,** 256–267 CrossRef Medline
118. Tanaka, G., Yamanaka, T., Furukawa, Y., Kajimura, N., Mitsuoka, K., and Nukina, N. (2019) Biochemical and morphological classification of disease-associated α-synuclein mutants aggregates. *Biochem. Biophys. Res. Commun.* **508,** 729–734 CrossRef Medline
119. Hwang, S., Fricke, P., Zinke, M., Giller, K., Wall, J. S., Riedel, D., Becker, S., and Lange, A. (2019) Comparison of the 3D structures of mouse and human α-synuclein fibrils by solid-state NMR and STEM. *J. Struct. Biol.* **206,** 43–48 CrossRef Medline
120. Luk, K. C., Covell, D. J., Kehm, V. M., Zhang, B., Song, I. Y., Byrne, M. D., Pitkin, R. M., Decker, S. C., Trojanowski, J. Q., and Lee, V. M.-Y. (2016) Molecular and biological compatibility with host α-synuclein influences fibril pathogenicity. *Cell Rep.* **16,** 3373–3387 CrossRef Medline
121. Lv, G., Kumar, A., Giller, K., Orcellet, M. L., Riedel, D., Fernández, C. O., Becker, S., and Lange, A. (2012) Structural comparison of mouse and human α-synuclein amyloid fibrils by solid-state NMR. *J. Mol. Biol.* **420,** 99–111 CrossRef Medline
122. Lv, G., Kumar, A., Huang, Y., and Eliezer, D. (2018) A protofilament-protofilament interface in the structure of mouse α-synuclein fibrils. *Biophys. J.* **114,** 2811–2819 CrossRef Medline
123. Mavroeidi, P., Arvanitaki, F., Karakitsou, A.-K., Vetsi, M., Kloukina, I., Zweckstetter, M., Giller, K., Becker, S., Sorrentino, Z. A., Giasson, B. I., Jensen, P. H., Stefanis, L., and Xilouri, M. (2019) Endogenous oligodendroglial α-synuclein and TPPP/p25α orchestrate α-synuclein pathology in experimental multiple system atrophy models. *Acta Neuropathol.* **138,** 415–441 CrossRef Medline
124. Muntané, G., Ferrer, I., and Martinez-Vicente, M. (2012) α-Synuclein phosphorylation and truncation are normal events in the adult human brain. *Neuroscience* **200,** 106–119 CrossRef Medline
125. Dunn, S. D. (1986) Effects of the modification of transfer buffer composition and the renaturation of proteins in gels on the recognition of proteins on Western blots by monoclonal antibodies. *Anal. Biochem.* **157,** 144–153 CrossRef Medline
126. Dickson, D. W., Liu, W., Hardy, J., Farrer, M., Mehta, N., Uitti, R., Mark, M., Zimmerman, T., Golbe, L., Sage, J., Sima, A., D'Amato, C., Albin, R., Gilman, S., and Yen, S. H. (1999) Widespread alterations of α-synuclein in multiple system atrophy. *Am. J. Pathol.* **155,** 1241–1251 CrossRef Medline
127. Tofaris, G. K., Razzaq, A., Ghetti, B., Lilley, K. S., and Spillantini, M. G. (2003) Ubiquitination of α-synuclein in Lewy bodies is a pathological event not associated with impairment of proteasome function. *J. Biol. Chem.* **278,** 44405–44411 CrossRef Medline
128. Dufty, B. M., Warner, L. R., Hou, S. T., Jiang, S. X., Gomez-Isla, T., Leenhouts, K. M., Oxford, J. T., Feany, M. B., Masliah, E., and Rohn, T. T. (2007) Calpain-cleavage of α-synuclein: connecting proteolytic processing to disease-linked aggregation. *Am. J. Pathol.* **170,** 1725–1738 CrossRef Medline
129. Lewis, K. A., Su, Y., Jou, O., Ritchie, C., Foong, C., Hynan, L. S., White, C. L., Thomas, P. J., and Hatanpaa, K. J. (2010) Abnormal neurites containing C-terminally truncated α-synuclein are present in Alzheimer's disease without conventional Lewy body pathology. *Am. J. Pathol.* **177,** 3037–3050 CrossRef Medline
130. Prasad, K., Beach, T. G., Hedreen, J., and Richfield, E. K. (2012) Critical role of truncated α-synuclein and aggregates in Parkinson's disease and

incidental Lewy body disease. *Brain Pathol.* **22,** 811–825 CrossRef Medline
131. Games, D., Seubert, P., Rockenstein, E., Patrick, C., Trejo, M., Ubhi, K., Ettle, B., Ghassemiam, M., Barbour, R., Schenk, D., Nuber, S., and Masliah, E. (2013) Axonopathy in an α-synuclein transgenic model of Lewy body disease is associated with extensive accumulation of C-terminal-truncated α-synuclein. *Am. J. Pathol.* **182,** 940–953 CrossRef Medline
132. Zhang, Z., Kang, S. S., Liu, X., Ahn, E. H., Zhang, Z., He, L., Iuvone, P. M., Duong, D. M., Seyfried, N. T., Benskey, M. J., Manfredsson, F. P., Jin, L., Sun, Y. E., Wang, J.-Z., and Ye, K. (2017) Asparagine endopeptidase cleaves α-synuclein and mediates pathologic activities in Parkinson's disease. *Nat. Struct. Mol. Biol.* **24,** 632–642 CrossRef Medline
133. Grassi, D., Howard, S., Zhou, M., Diaz-Perez, N., Urban, N. T., Guerrero-Given, D., Kamasawa, N., Volpicelli-Daley, L. A., LoGrasso, P., and Lasmézas, C. I. (2018) Identification of a highly neurotoxic α-synuclein species inducing mitochondrial damage and mitophagy in Parkinson's disease. *Proc. Natl. Acad. Sci. U. S. A.* **115,** E2634–E2643 CrossRef Medline
134. Killinger, B. A., Madaj, Z., Sikora, J. W., Rey, N., Haas, A. J., Vepa, Y., Lindqvist, D., Chen, H., Thomas, P. M., Brundin, P., Brundin, L., and Labrie, V. (2018) The vermiform appendix impacts the risk of developing Parkinson's disease. *Sci. Transl. Med.* **10,** eaar5280 CrossRef Medline
135. Ahn, E. H., Kang, S. S., Liu, X., Chen, G., Zhang, Z., Chandrasekharan, B., Alam, A. M., Neish, A. S., Cao, X., and Ye, K. (2020) Initiation of Parkinson's disease from gut to brain by δ-secretase. *Cell Res.* **30,** 70–87 CrossRef Medline
136. Kovacs, G. G., Wagner, U., Dumont, B., Pikkarainen, M., Osman, A. A., Streichenberger, N., Leisser, I., Verchère, J., Baron, T., Alafuzoff, I., Budka, H., Perret-Liaudet, A., and Lachmann, I. (2012) An antibody with high reactivity for disease-associated α-synuclein reveals extensive brain pathology. *Acta Neuropathol.* **124,** 37–50 CrossRef Medline
137. Braak, H., Sastre, M., and Del Tredici, K. (2007) Development of α-synuclein immunoreactive astrocytes in the forebrain parallels stages of intraneuronal pathology in sporadic Parkinson's disease. *Acta Neuropathol.* **114,** 231–241 CrossRef Medline
138. Kovacs, G. G., Breydo, L., Green, R., Kis, V., Puska, G., Lőrincz, P., Perju-Dumbrava, L., Giera, R., Pirker, W., Lutz, M., Lachmann, I., Budka, H., Uversky, V. N., Molnár, K., and László, L. (2014) Intracellular processing of disease-associated α-synuclein in the human brain suggests prion-like cell-to-cell spread. *Neurobiol. Dis.* **69,** 76–92 CrossRef Medline
139. Gámez-Valero, A., and Beyer, K. (2018) Alternative splicing of α- and β-synuclein genes plays differential roles in synucleinopathies. *Genes (Basel)* **9,** E63 CrossRef Medline
140. Lee, M. K., Stirling, W., Xu, Y., Xu, X., Qui, D., Mandir, A. S., Dawson, T. M., Copeland, N. G., Jenkins, N. A., and Price, D. L. (2002) Human α-synuclein-harboring familial Parkinson's disease-linked Ala-53-Thr mutation causes neurodegenerative disease with α-synuclein aggregation in transgenic mice. *Proc. Natl. Acad. Sci. U. S. A.* **99,** 8968–8973 CrossRef Medline
141. McGlinchey, R. P., Lacy, S. M., Huffer, K. E., Tayebi, N., Sidransky, E., and Lee, J. C. (2019) C-terminal α-synuclein truncations are linked to cysteine cathepsin activity in Parkinson's disease. *J. Biol. Chem.* **294,** 9973–9984 CrossRef Medline
142. Izawa, Y., Tateno, H., Kameda, H., Hirakawa, K., Hato, K., Yagi, H., Hongo, K., Mizobata, T., and Kawata, Y. (2012) Role of C-terminal negative charges and tyrosine residues in fibril formation of α-synuclein. *Brain Behav.* **2,** 595–605 CrossRef Medline
143. Afitska, K., Fucikova, A., Shvadchak, V. V., and Yushchenko, D. A. (2017) Modification of C terminus provides new insights into the mechanism of α-synuclein aggregation. *Biophys. J.* **113,** 2182–2191 CrossRef Medline
144. Uversky, V. N., Gillespie, J. R., and Fink, A. L. (2000) Why are "natively unfolded" proteins unstructured under physiologic conditions? *Proteins* **41,** 415–427 CrossRef Medline
145. Hashimoto, M., Hsu, L. J., Sisk, A., Xia, Y., Takeda, A., Sundsmo, M., and Masliah, E. (1998) Human recombinant NACP/α-synuclein is aggregated and fibrillated *in vitro*: relevance for Lewy body disease. *Brain Res.* **799,** 301–306 CrossRef Medline
146. Paik, S. R., Shin, H. J., Lee, J. H., Chang, C. S., and Kim, J. (1999) Copper (II)-induced self-oligomerization of α-synuclein. *Biochem. J.* **340,** 821–828 CrossRef Medline
147. Uversky, V. N., Li, J., and Fink, A. L. (2001) Evidence for a partially folded intermediate in α-synuclein fibril formation. *J. Biol. Chem.* **276,** 10737–10744 CrossRef Medline
148. Nielsen, M. S., Vorum, H., Lindersson, E., and Jensen, P. H. (2001) Ca^{2+} binding to α-synuclein regulates ligand binding and oligomerization. *J. Biol. Chem.* **276,** 22680–22684 CrossRef Medline
149. Lowe, R., Pountney, D. L., Jensen, P. H., Gai, W. P., and Voelcker, N. H. (2004) Calcium(II) selectively induces α-synuclein annular oligomers via interaction with the C-terminal domain. *Protein Sci.* **13,** 3245–3252 CrossRef Medline
150. Trexler, A. J., and Rhoades, E. (2010) Single molecule characterization of α-synuclein in aggregation-prone states. *Biophys. J.* **99,** 3048–3055 CrossRef Medline
151. Park, S. M., Jung, H. Y., Chung, K. C., Rhim, H., Park, J. H., and Kim, J. (2002) Stress-induced aggregation profiles of GST-α-synuclein fusion proteins: role of the C-terminal acidic tail of α-synuclein in protein thermosolubility and stability. *Biochemistry* **41,** 4137–4146 CrossRef Medline
152. McLean, P. J., and Hyman, B. T. (2002) An alternatively spliced form of rodent alpha-synuclein forms intracellular inclusions *in vitro*: role of the carboxy-terminus in α-synuclein aggregation. *Neurosci. Lett.* **323,** 219–223 CrossRef Medline
153. Bertoncini, C. W., Jung, Y.-S., Fernandez, C. O., Hoyer, W., Griesinger, C., Jovin, T. M., and Zweckstetter, M. (2005) Release of long-range tertiary interactions potentiates aggregation of natively unstructured α-synuclein. *Proc. Natl. Acad. Sci. U. S. A.* **102,** 1430–1435 CrossRef Medline
154. Yap, T. L., Pfefferkorn, C. M., and Lee, J. C. (2011) Residue-specific fluorescent probes of α-synuclein: detection of early events at the N- and C-termini during fibril assembly. *Biochemistry* **50,** 1963–1965 CrossRef Medline
155. Park, S., Yoon, J., Jang, S., Lee, K., and Shin, S. (2016) The role of the acidic domain of α-synuclein in amyloid fibril formation: a molecular dynamics study. *J. Biomol. Struct. Dyn.* **34,** 376–383 CrossRef Medline
156. El-Turk, F., Newby, F. N., De Genst, E., Guilliams, T., Sprules, T., Mittermaier, A., Dobson, C. M., and Vendruscolo, M. (2016) Structural effects of two camelid nanobodies directed to distinct C-terminal epitopes on α-synuclein. *Biochemistry* **55,** 3116–3122 CrossRef Medline
157. Baul, U., Chakraborty, D., Mugnai, M. L., Straub, J. E., and Thirumalai, D. (2019) Sequence effects on size, shape, and structural heterogeneity in intrinsically disordered proteins. *J. Phys. Chem. B* **123,** 3462–3474 CrossRef Medline
158. Meuvis, J., Gerard, M., Desender, L., Baekelandt, V., and Engelborghs, Y. (2010) The conformation and the aggregation kinetics of α-synuclein depend on the proline residues in its C-terminal region. *Biochemistry* **49,** 9345–9352 CrossRef Medline
159. Sorrentino, Z. A., Xia, Y., Gorion, K., Hass, E., and Giasson, B. I. (2020) Carboxy-terminal truncations of mouse α-synuclein alter aggregation and prion-like seeding. *FEBS Lett.* **594,** 1271–1283 CrossRef Medline
160. Ma, L., Yang, C., Zhang, X., Li, Y., Wang, S., Zheng, L., and Huang, K. (2018) C-terminal truncation exacerbates the aggregation and cytotoxicity of α-synuclein: a vicious cycle in Parkinson's disease. *Biochim. Biophys. Acta Mol. Basis Dis.* **1864,** 3714–3725 CrossRef Medline
161. Ni, X., McGlinchey, R. P., Jiang, J., and Lee, J. C. (2019) Structural insights into α-synuclein fibril polymorphism: effects of Parkinson's disease-related C-terminal truncations. *J. Mol. Biol.* **431,** 3913–3919 CrossRef Medline
162. Wang, W., Nguyen, L. T. T., Burlak, C., Chegini, F., Guo, F., Chataway, T., Ju, S., Fisher, O. S., Miller, D. W., Datta, D., Wu, F., Wu, C. X., Landeru, A., Wells, J. A., Cookson, M. R., *et al.* (2016) Caspase-1 causes truncation and aggregation of the Parkinson's disease-associated protein α-synuclein. *Proc. Natl. Acad. Sci. U. S. A.* **113,** 9587–9592 CrossRef Medline
163. van der Wateren, I. M., Knowles, T. P. J., Buell, A. K., Dobson, C. M., and Galvagnion, C. (2018) C-terminal truncation of α-synuclein promotes

amyloid fibril amplification at physiological pH. *Chem. Sci.* **9,** 5506–5516 CrossRef Medline

164. Levin, J., Giese, A., Boetzel, K., Israel, L., Högen, T., Nübling, G., Kretzschmar, H., and Lorenzl, S. (2009) Increased α-synuclein aggregation following limited cleavage by certain matrix metalloproteinases. *Exp. Neurol.* **215,** 201–208 CrossRef Medline
165. Zibaee, S., Jakes, R., Fraser, G., Serpell, L. C., Crowther, R. A., and Goedert, M. (2007) Sequence determinants for amyloid fibrillogenesis of human alpha-synuclein. *J. Mol. Biol.* **374,** 454–464 CrossRef Medline
166. Vamvaca, K., Lansbury, P. T., Jr., and Stefanis, L. (2011) N-terminal deletion does not affect α-synuclein membrane binding, self-association and toxicity in human neuroblastoma cells, unlike yeast. *J. Neurochem.* **119,** 389–397 CrossRef Medline
167. Kessler, J. C., Rochet, J. C., and Lansbury, P. T. (2003) The N-terminal repeat domain of α-synuclein inhibits β-sheet and amyloid fibril formation. *Biochemistry* **42,** 672–678 CrossRef Medline
168. Sung, J. Y., Park, S. M., Lee, C.-H., Um, J. W., Lee, H. J., Kim, J., Oh, Y. J., Lee, S.-T., Paik, S. R., and Chung, K. C. (2005) Proteolytic cleavage of extracellular secreted {alpha}-synuclein via matrix metalloproteinases. *J. Biol. Chem.* **280,** 25216–25224 CrossRef Medline
169. Cuervo, A. M., Stefanis, L., Fredenburg, R., Lansbury, P. T., and Sulzer, D. (2004) Impaired degradation of mutant α-synuclein by chaperone-mediated autophagy. *Science* **305,** 1292–1295 CrossRef Medline
170. Sugeno, N., Hasegawa, T., Tanaka, N., Fukuda, M., Wakabayashi, K., Oshima, R., Konno, M., Miura, E., Kikuchi, A., Baba, T., Anan, T., Nakao, M., Geisler, S., Aoki, M., and Takeda, A. (2014) Lys-63-linked ubiquitination by E3 ubiquitin ligase Nedd4-1 facilitates endosomal sequestration of internalized α-synuclein. *J. Biol. Chem.* **289,** 18137–18151 CrossRef Medline
171. Jia, C., Ma, X., Liu, Z., Gu, J., Zhang, X., Li, D., and Zhang, S. (2019) Different heat shock proteins bind α-synuclein with distinct mechanisms and synergistically prevent its amyloid aggregation. *Front. Neurosci.* **13,** 1124 CrossRef Medline
172. Norris, E. H., Giasson, B. I., Hodara, R., Xu, S., Trojanowski, J. Q., Ischiropoulos, H., and Lee, V. M.-Y. (2005) Reversible inhibition of α-synuclein fibrillization by dopaminochrome-mediated conformational alterations. *J. Biol. Chem.* **280,** 21212–21219 CrossRef Medline
173. Mazzulli, J. R., Armakola, M., Dumoulin, M., Parastatidis, I., and Ischiropoulos, H. (2007) Cellular oligomerization of α-synuclein is determined by the interaction of oxidized catechols with a C-terminal sequence. *J. Biol. Chem.* **282,** 31621–31630 CrossRef Medline
174. Hall, K., Yang, S., Sauchanka, O., Spillantini, M. G., and Anichtchik, O. (2015) Behavioural deficits in transgenic mice expressing human truncated (1-120 amino acid) α-synuclein. *Exp. Neurol.* **264,** 8–13 CrossRef Medline
175. Bungeroth, M., Appenzeller, S., Regulin, A., Völker, W., Lorenzen, I., Grötzinger, J., Pendziwiat, M., and Kuhlenbäumer, G. (2014) Differential aggregation properties of alpha-synuclein isoforms. *Neurobiol. Aging.* **35,** 1913–1919 CrossRef Medline
176. Ma, K.-L., Song, L.-K., Long, W. A., Yuan, Y.-H., Zhang, Y., Song, X.-Y., Niu, F., Han, N., and Chen, N.-H. (2013) Deletion in exon 5 of the SNCA gene and exposure to rotenone leads to oligomerization of α-synuclein and toxicity to PC12 cells. *Brain. Res. Bull.* **90,** 127–131 CrossRef Medline
177. Stefanova, N., Klimaschewski, L., Poewe, W., Wenning, G. K., and Reindl, M. (2001) Glial cell death induced by overexpression of α-synuclein. *J. Neurosci. Res.* **65,** 432–438 CrossRef Medline
178. Stefanova, N., Emgård, M., Klimaschewski, L., Wenning, G. K., and Reindl, M. (2002) Ultrastructure of α-synuclein-positive aggregations in U373 astrocytoma and rat primary glial cells. *Neurosci. Lett.* **323,** 37–40 CrossRef Medline
179. Tofaris, G. K., Garcia Reitböck, P., Humby, T., Lambourne, S. L., O'Connell, M., Ghetti, B., Gossage, H., Emson, P. C., Wilkinson, L. S., Goedert, M., and Spillantini, M. G. (2006) Pathological changes in dopaminergic nerve cells of the substantia nigra and olfactory bulb in mice transgenic for truncated human α-synuclein(1-120): implications for Lewy body disorders. *J. Neurosci.* **26,** 3942–3950 CrossRef Medline
180. Periquet, M., Fulga, T., Myllykangas, L., Schlossmacher, M. G., and Feany, M. B. (2007) Aggregated α-synuclein mediates dopaminergic neurotoxicity *in vivo*. *J. Neurosci.* **27,** 3338–3346 CrossRef Medline
181. Garcia-Reitböck, P., Anichtchik, O., Bellucci, A., Iovino, M., Ballini, C., Fineberg, E., Ghetti, B., Della Corte, L., Spano, P., Tofaris, G. K., Goedert, M., and Spillantini, M. G. (2010) SNARE protein redistribution and synaptic failure in a transgenic mouse model of Parkinson's disease. *Brain* **133,** 2032–2044 CrossRef Medline
182. Ulusoy, A., Febbraro, F., Jensen, P. H., Kirik, D., and Romero-Ramos, M. (2010) Co-expression of C-terminal truncated α-synuclein enhances full-length α-synuclein-induced pathology. *Eur. J. Neurosci.* **32,** 409–422 CrossRef Medline
183. Fares, M.-B., Maco, B., Oueslati, A., Rockenstein, E., Ninkina, N., Buchman, V. L., Masliah, E., and Lashuel, H. A. (2016) Induction of *de novo* α-synuclein fibrillization in a neuronal model for Parkinson's disease. *Proc. Natl. Acad. Sci. U. S. A.* **113,** E912–E921 CrossRef Medline
184. Wakamatsu, M., Ishii, A., Iwata, S., Sakagami, J., Ukai, Y., Ono, M., Kanbe, D., Muramatsu, S., Kobayashi, K., Iwatsubo, T., and Yoshimoto, M. (2008) Selective loss of nigral dopamine neurons induced by overexpression of truncated human α-synuclein in mice. *Neurobiol. Aging* **29,** 574–585 CrossRef Medline
185. Daher, J. P. L., Ying, M., Banerjee, R., McDonald, R. S., Hahn, M. D., Yang, L., Flint Beal, M., Thomas, B., Dawson, V. L., Dawson, T. M., and Moore, D. J. (2009) Conditional transgenic mice expressing C-terminally truncated human α-synuclein (αSyn119) exhibit reduced striatal dopamine without loss of nigrostriatal pathway dopaminergic neurons. *Mol. Neurodegener.* **4,** 34 CrossRef Medline
186. Choi, D.-H., Kim, Y.-J., Kim, Y.-G., Joh, T. H., Beal, M. F., and Kim, Y.-S. (2011) Role of matrix metalloproteinase 3-mediated α-synuclein cleavage in dopaminergic cell death. *J. Biol. Chem.* **286,** 14168–14177 CrossRef Medline
187. Anderson, V. L., Ramlall, T. F., Rospigliosi, C. C., Webb, W. W., and Eliezer, D. (2010) Identification of a helical intermediate in trifluoroethanol-induced α-synuclein aggregation. *Proc. Natl. Acad. Sci. U. S. A.* **107,** 18850–18855 CrossRef Medline
188. Li, H.-T., Du, H.-N., Tang, L., Hu, J., and Hu, H.-Y. (2002) Structural transformation and aggregation of human α-synuclein in trifluoroethanol: non-amyloid component sequence is essential and β-sheet formation is prerequisite to aggregation. *Biopolymers* **64,** 221–226 CrossRef Medline
189. Terada, M., Suzuki, G., Nonaka, T., Kametani, F., Tamaoka, A., and Hasegawa, M. (2018) The effect of truncation on prion-like properties of α-synuclein. *J. Biol. Chem.* **293,** 13910–13920 CrossRef Medline
190. Guerrero-Ferreira, R., Taylor, N. M., Mona, D., Ringler, P., Lauer, M. E., Riek, R., Britschgi, M., and Stahlberg, H. (2018) Cryo-EM structure of α-synuclein fibrils. *Elife* **7,** e36402 CrossRef Medline
191. Li, B., Ge, P., Murray, K. A., Sheth, P., Zhang, M., Nair, G., Sawaya, M. R., Shin, W. S., Boyer, D. R., Ye, S., Eisenberg, D. S., Zhou, Z. H., and Jiang, L. (2018) Cryo-EM of full-length α-synuclein reveals fibril polymorphs with a common structural kernel. *Nat. Commun.* **9,** 3609 CrossRef Medline
192. Sacino, A. N., Brooks, M. M., Chakrabarty, P., Saha, K., Khoshbouei, H., Golde, T. E., and Giasson, B. I. (2017) Proteolysis of α-synuclein fibrils in the lysosomal pathway limits induction of inclusion pathology. *J. Neurochem.* **140,** 662–678 CrossRef Medline
193. Qiang, W., Yau, W. M., Lu, J. X., Collinge, J., and Tycko, R. (2017) Structural variation in amyloid-β fibrils from Alzheimer's disease clinical subtypes. *Nature* **541,** 217–221 CrossRef Medline
194. Jang, A., Lee, H.-J., Suk, J.-E., Jung, J.-W., Kim, K.-P., and Lee, S.-J. (2010) Non-classical exocytosis of α-synuclein is sensitive to folding states and promoted under stress conditions. *J. Neurochem.* **113,** 1263–1274 CrossRef Medline
195. Bieri, G., Gitler, A. D., and Brahic, M. (2018) Internalization, axonal transport and release of fibrillar forms of α-synuclein. *Neurobiol. Dis.* **109,** 219–225 CrossRef Medline
196. Nam, M.-K., Han, J.-H., Jang, J.-Y., Yun, S.-E., Kim, G.-Y., Kang, S., and Rhim, H. (2015) A novel link between the conformations, exposure of specific epitopes, and subcellular localization of α-synuclein. *Biochim. Biophys. Acta* **1850,** 2497–2505 CrossRef Medline

197. Tanik, S. A., Schultheiss, C. E., Volpicelli-Daley, L. A., Brunden, K. R., and Lee, V. M. Y. (2013) Lewy body-like α-synuclein aggregates resist degradation and impair macroautophagy. *J. Biol. Chem.* **288,** 15194–15210 CrossRef Medline
198. Luk, K. C., Song, C., O'Brien, P., Stieber, A., Branch, J. R., Brunden, K. R., Trojanowski, J. Q., and Lee, V. M.-Y. (2009) Exogenous α-synuclein fibrils seed the formation of Lewy body-like intracellular inclusions in cultured cells. *Proc. Natl. Acad. Sci. U. S. A.* **106,** 20051–20056 CrossRef Medline
199. Sacino, A. N., Brooks, M., Thomas, M. A., McKinney, A. B., McGarvey, N. H., Rutherford, N. J., Ceballos-Diaz, C., Robertson, J., Golde, T. E., and Giasson, B. I. (2014) Amyloidogenic α-synuclein seeds do not invariably induce rapid, widespread pathology in mice. *Acta Neuropathol.* **127,** 645–665 CrossRef Medline
200. Fellner, L., Irschick, R., Schanda, K., Reindl, M., Klimaschewski, L., Poewe, W., Wenning, G. K., and Stefanova, N. (2013) Toll-like receptor 4 is required for alpha-synuclein dependent activation of microglia and astroglia. *Glia* **61,** 349–360 CrossRef Medline
201. Kanda, S., Bishop, J. F., Eglitis, M. A., Yang, Y., and Mouradian, M. M. (2000) Enhanced vulnerability to oxidative stress by α-synuclein mutations and C-terminal truncation. *Neuroscience* **97,** 279–284 CrossRef Medline
202. Michell, A. W., Tofaris, G. K., Gossage, H., Tyers, P., Spillantini, M. G., and Barker, R. A. (2007) The effect of truncated human alpha-synuclein (1-120) on dopaminergic cells in a transgenic mouse model of Parkinson's disease. *Cell Transplant.* **16,** 461–474 CrossRef Medline
203. Surmeier, D. J. (2018) Determinants of dopaminergic neuron loss in Parkinson's disease. *FEBS J.* **285,** 3657–3668 CrossRef Medline
204. Stefanis, L., Emmanouilidou, E., Pantazopoulou, M., Kirik, D., Vekrellis, K., and Tofaris, G. K. (2019) How is alpha-synuclein cleared from the cell? *J. Neurochem.* **150,** 577–590 CrossRef Medline
205. Bennett, M. C., Bishop, J. F., Leng, Y., Chock, P. B., Chase, T. N., and Mouradian, M. M. (1999) Degradation of α-synuclein by proteasome. *J. Biol. Chem.* **274,** 33855–33858 CrossRef
206. Iwata, A., Maruyama, M., Akagi, T., Hashikawa, T., Kanazawa, I., Tsuji, S., and Nukina, N. (2003) α-Synuclein degradation by serine protease neurosin: implication for pathogenesis of synucleinopathies. *Hum. Mol. Genet.* **12,** 2625–2635 CrossRef Medline
207. Kasai, T., Tokuda, T., Yamaguchi, N., Watanabe, Y., Kametani, F., Nakagawa, M., and Mizuno, T. (2008) Cleavage of normal and pathological forms of α-synuclein by neurosin *in vitro*. *Neurosci. Lett.* **436,** 52–56 CrossRef Medline
208. Tatebe, H., Watanabe, Y., Kasai, T., Mizuno, T., Nakagawa, M., Tanaka, M., and Tokuda, T. (2010) Extracellular neurosin degrades α-synuclein in cultured cells. *Neurosci. Res.* **67,** 341–346 CrossRef Medline
209. Spencer, B., Michael, S., Shen, J., Kosberg, K., Rockenstein, E., Patrick, C., Adame, A., and Masliah, E. (2013) Lentivirus mediated delivery of neurosin promotes clearance of wild-type α-synuclein and reduces the pathology in an α-synuclein model of LBD. *Mol. Ther.* **21,** 31–41 CrossRef Medline
210. Spencer, B., Valera, E., Rockenstein, E., Trejo-Morales, M., Adame, A., and Masliah, E. (2015) A brain-targeted, modified neurosin (kallikrein-6) reduces α-synuclein accumulation in a mouse model of multiple system atrophy. *Mol. Neurodegener.* **10,** 48 CrossRef Medline
211. Pampalakis, G., Sykioti, V. S., Ximerakis, M., Stefanakou-Kalakou, I., Melki, R., Vekrellis, K., and Sotiropoulou, G. (2017) KLK6 proteolysis is implicated in the turnover and uptake of extracellular α-synuclein species. *Oncotarget* **8,** 14502–14515 CrossRef Medline
212. Oh, S. H., Kim, H. N., Park, H. J., Shin, J. Y., Kim, D. Y., and Lee, P. H. (2017) The cleavage effect of mesenchymal stem cell and its derived matrix metalloproteinase-2 on extracellular α-synuclein aggregates in parkinsonian models. *Stem Cells Transl. Med.* **6,** 949–961 CrossRef Medline
213. Kim, K. S., Choi, Y. R., Park, J.-Y., Lee, J.-H., Kim, D. K., Lee, S.-J., Paik, S. R., Jou, I., and Park, S. M. (2012) Proteolytic cleavage of extracellular α-synuclein by plasmin: implications for Parkinson disease. *J. Biol. Chem.* **287,** 24862–24872 CrossRef Medline
214. Takahashi, M., Ko, L., Kulathingal, J., Jiang, P., Sevlever, D., and Yen, S.-H. C. (2007) Oxidative stress-induced phosphorylation, degradation and aggregation of α-synuclein are linked to upregulated CK2 and cathepsin D. *Eur. J. Neurosci.* **26,** 863–874 CrossRef Medline
215. McGlinchey, R. P., Dominah, G. A., and Lee, J. C. (2017) Taking a bite out of amyloid: mechanistic insights into α-synuclein degradation by cathepsin L. *Biochemistry* **56,** 3881–3884 CrossRef Medline
216. McNaught, K. S., and Jenner, P. (2001) Proteasomal function is impaired in substantia nigra in Parkinson's disease. *Neurosci. Lett.* **297,** 191–194 CrossRef Medline
217. Crocker, S. J., Smith, P. D., Jackson-Lewis, V., Lamba, W. R., Hayley, S. P., Grimm, E., Callaghan, S. M., Slack, R. S., Melloni, E., Przedborski, S., Robertson, G. S., Anisman, H., Merali, Z., and Park, D. S. (2003) Inhibition of calpains prevents neuronal and behavioral deficits in an MPTP mouse model of Parkinson's disease. *J. Neurosci.* **23,** 4081–4091 CrossRef Medline
218. Diepenbroek, M., Casadei, N., Esmer, H., Saido, T. C., Takano, J., Kahle, P. J., Nixon, R. A., Rao, M. V., Melki, R., Pieri, L., Helling, S., Marcus, K., Krueger, R., Masliah, E., Riess, O., *et al.* (2014) Overexpression of the calpain-specific inhibitor calpastatin reduces human α-synuclein processing, aggregation and synaptic impairment in [A30P]αSyn transgenic mice. *Hum. Mol. Genet.* **23,** 3975–3989 CrossRef Medline
219. Hassen, G. W., Kesner, L., Stracher, A., Shulman, A., Rockenstein, E., Mante, M., Adame, A., Overk, C., Rissman, R. A., and Masliah, E. (2018) Effects of novel calpain inhibitors in transgenic animal model of Parkinson's disease/dementia with Lewy bodies. *Sci. Rep.* **8,** 18083 CrossRef Medline
220. Bassil, F., Fernagut, P. O., Bezard, E., Pruvost, A., Leste-Lasserre, T., Hoang, Q. Q., Ringe, D., Petsko, G. A., and Meissner, W. G. (2016) Reducing C-terminal truncation mitigates synucleinopathy and neurodegeneration in a transgenic model of multiple system atrophy. *Proc. Natl. Acad. Sci. U. S. A.* **113,** 9593–9598 CrossRef Medline
221. Gan, L., Vargas, M. R., Johnson, D. A., and Johnson, J. A. (2012) Astrocyte-specific overexpression of Nrf2 delays motor pathology and synuclein aggregation throughout the CNS in the α-synuclein mutant (A53T) mouse model. *J. Neurosci.* **32,** 17775–17787 CrossRef Medline
222. Ferree, A. W. (2019) Cathepsin oxidation alters α-synuclein processing. *Front. Neurol.* **10,** 530 CrossRef Medline
223. Korovila, I., Hugo, M., Castro, J. P., Weber, D., Höhn, A., Grune, T., and Jung, T. (2017) Proteostasis, oxidative stress and aging. *Redox Biol.* **13,** 550–567 CrossRef Medline
224. Malkus, K. A., and Ischiropoulos, H. (2012) Regional deficiencies in chaperone-mediated autophagy underlie α-synuclein aggregation and neurodegeneration. *Neurobiol. Dis.* **46,** 732–744 CrossRef Medline
225. Senkevich, K., and Gan-Or, Z. (2019) Autophagy lysosomal pathway dysfunction in Parkinson's disease; evidence from human genetics. *Parkinsonism Relat. Disord.* CrossRef Medline
226. Lehtonen, Š., Sonninen, T.-M., Wojciechowski, S., Goldsteins, G., and Koistinaho, J. (2019) Dysfunction of cellular proteostasis in Parkinson's disease. *Front. Neurosci.* **13,** 457 CrossRef Medline
227. Games, D., Valera, E., Spencer, B., Rockenstein, E., Mante, M., Adame, A., Patrick, C., Ubhi, K., Nuber, S., Sacayon, P., Zago, W., Seubert, P., Barbour, R., Schenk, D., and Masliah, E. (2014) Reducing C-terminal-truncated alpha-synuclein by immunotherapy attenuates neurodegeneration and propagation in Parkinson's disease-like models. *J. Neurosci* **34,** 9441–9454 CrossRef Medline